Received: 2 November 2018 | Revised: 28 January 2019 | Accepted: 7 February 2019

DOI: 10.1002/cnr2.1169

REVIEW

WILEY Cancer Reports

Comparison of prostate-specific membrane antigen ligands in clinical translation research for diagnosis of prostate cancer

Sagnik Sengupta[1] | Mena Asha Krishnan[2] | Sudeshna Chattopadhyay[2,3,4] | Venkatesh Chelvam[1,2]

[1] Discipline of Chemistry, School of Basic Sciences, Indian Institute of Technology Indore, Indore, India

[2] Discipline of Biosciences and Biomedical Engineering, School of Engineering, Indian Institute of Technology Indore, Indore, India

[3] Discipline of Physics, School of Basic Sciences, Indian Institute of Technology Indore, Indore, India

[4] Discipline of Metallurgy Engineering and Material Science, School of Engineering, Indian Institute of Technology Indore, Indore, India

Correspondence
Venkatesh Chelvam, Discipline of Chemistry, School of Basic Sciences, Indian Institute of Technology Indore, Simrol, Indore 453 552, India.
Email: cvenkat@iiti.ac.in

Sudeshna Chattopadhyay, Discipline of Biosciences and Biomedical Engineering, School of Engineering, Simrol, Indore 453 552, India.
Email: sudeshna@iiti.ac.in

Funding information
Indian Institute of Technology (IIT) Indore, India; Ministry of Human Resource Development (MHRD), Government of India

Abstract

Background: Prostate-specific membrane antigen (PSMA), overexpressed on prostate cancer (PCa), is a well-characterized cell surface protein to selectively diagnose PCa. PSMA's unique characteristics and its 1000-fold higher expression in PCa compared with other tissues renders it as a suitable biomarker for detection of PCa in its early stage. In this report, we critically analyze and recommend the requirements needed for the development of variety of PSMA-targeted molecular imaging agents based on antibodies, small molecule ligands, peptides, and aptamers. The targeting moieties are either conjugated to radionuclear isotopes or near-infrared agents for efficient diagnosis of PCa.

Recent findings: From the analysis, it was found that several small molecule–derived PCa imaging agents are approved for clinical trials in Europe and the United States, and few are already in the clinical use for diagnosis of PCa. Even though ^{111}In-labeled capromab pendetide was approved by the Food and Drug Administration (FDA) and other engineered antibodies are available for detection of PCa, but high production cost, low shelf life (less than 1 month at 4°C), possibility of human immuno reactions, and low blood clearance rate necessitated a need for developing new imaging agents, which are serum stable, cost-effective, and possesses longer shelf life (6 months), have fast clearance rate from nontargeted tissues during the diagnosis process. It is found that small molecule ligand-derived imaging agents possesses most of the desired properties expected for an ideal diagnostic agent when compared with other targeting moieties.

List of abbreviations: [^{18}F]DCFPyL, 2-(3-{1-carboxy-5-[(6-[^{18}F]fluoropyridine-3-carbonyl)-amino]-pentyl}-ureido)-pentanedioic acid; [^{18}F]FECH, fluoroethylcholine; [^{18}F]FMCH, fluoromethylcholine; BPH, benign prostatic hyperplasia; CB-TE2A, 4,11-bis (carboxymethyl)-1,4,8,11-tetraazabicyclo[6.6.2]hexadecane; CT, computed tomography; CTCs, circulating tumor cells; Cys-CO-Glu, (*S*)-2-[3-[(*R*)-1-carboxy-2-mercaptoethyl]ureido-pentanedioic acid; DCFBC, *N*-[*N*-[(*S*)-1,3-dicarboxypropyl]carbamoyl]-4-[^{18}F]fluorobenzyl-L-cysteine; DCIT, *N*-[*N*-[(*S*)-1,3-dicarboxypropyl]carbamoyl]-S-3-[^{125}I]iodo-L-tyrosine; DCMC, *N*-[*N*-[(*S*)-1,3-dicarboxypropyl]carbamoyl]-S-[^{11}C]methyl-L-cysteine; DKFZ-PSMA-617, deutsche krebs forschung zentrum–prostate-specific membrane antigen; DOTA, 1,4,7,10-tetraazacyclododecane-1,4,7,10-tetraacetic acid; DRE, digital rectal exam; DUPA, 2-[3-(1,3-dicarboxypropyl)ureido]pentanedioic acid; EPR, enhanced permeability and retention effect; FDA, Food and Drug Administration; GPI, glycosylphosphatidylinositol; GYK-DTPA, glycyl-tyrosyl-(*N*,ε-diethylenetriaminepentaacetic acid)-lysine; HAMA, human anti-mouse antibodies; HBED-CC, *N*,*N*′-bis[2-hydroxy-5-(carboxyethyl)benzyl] ethylenediamine-*N*,*N*′-diacetic acid; ID/g, injected dose per gram; IgG1, human immunoglobulin G1; LNCaP, lymph node prostate cancer; mAb, monoclonal antibody; MAS_3, *S*-acetylmercaptoacetyltriserine; MIP-1072, [(*S*)-2-(3-((*S*)-1-carboxy-5-(4-iodobenzylamino)pentyl) ureido)pentanedioic acid]; MIP-1095, [*S*)-2-(3-((*S*)-1-carboxy-5-(3-(4-iodophenyl)ureido)pentyl)ureido)pentanedioic acid]; MRI, magnetic resonance imaging; MRS, magnetic resonance spectroscopy; MRSI, magnetic resonance spectroscopic imaging; NAAG, N-acetyl-aspartyl-glutamate; NAALADase, *N*-acetylated alpha-linked acidic dipeptidase; NHS, *N*-hydroxysuccinimide ester; NIR, near-infrared; NOTA, 1,4,7-triazacyclononane-1,4,7-triacetic acid; Oxo-DO3A, 1-oxa-4,7,10-triazacyclododecane-4,7,10-triacetic acid; PAP, prostatic acid phosphatase; PCa, prostate cancer; PCTA, 3,6,9,15-tetraazabicyclo[9.3.1]pentadeca-1(15),11,13-triene-3,6,9-triacetic acid; PDD, intraoperative photodiagnosis; PET, positron emission tomography; PLND, pelvic lymph node dissection; PSA, prostate-specific antigen; PSCA, prostate stem cell antigen; PSM, positive surgical margins; PSMA, prostate-specific membrane antigen; PSMA-I&T, prostate-specific membrane antigen–imaging and therapy; QD, quantum dot; QD-Apt-Drug, QD-aptamer-drug conjugate; SCID, severe combined immunodeficiency; SELEX, systematic evolution of ligands by exponential enrichment; SPECT, single photon emission computed tomography; SPION, superparamagnetic iron oxide nanoparticles; TRUS, transrectal ultrasound

Conclusion: This report discusses in detail the homing moieties used in the development of targeted diagnostic tools for detection of PCa. The merits and demerits of monoclonal antibodies, small molecule ligands, peptides, and aptamers for imaging of PCa and intraoperative guided surgery are extensively analyzed. Among all, urea-based ligands were found to be most successful in preclinical and clinical trials and show a major promise for future commercialization.

KEYWORDS

biomarker, diagnosis, near-infrared imaging, prostate cancer, PSMA, radionuclear imaging

1 | INTRODUCTION

Unification of molecular biology and in vivo imaging resulted in the advent of a new discipline popularly known as "molecular imaging" in the field of medical diagnosis. It allows the visualization of the cellular functions and dynamic molecular processes in living cells noninvasively. The unique ability of this new technique allows it a multifarious entry into the field of disease diagnosis especially in cancer, inflammatory, neurological, and cardiovascular diseases.

Conventional imaging techniques such as X-ray, ultrasound, computed tomography (CT), and magnetic resonance imaging (MRI) can detect only morphological and anatomical changes in organs and tissues and often fail to distinguish abnormalities arising due to inflammatory and pathological diseases.[1] In molecular imaging, targeted or nontargeted "radiolabeled or fluorescent tracers" are systemically introduced into the biological system and monitored for their ready uptake by abnormal or hyperactive tissues. Abnormal cells overexpress special cell surface proteins that are anchored on the plasma membrane of the cells during diseased conditions. These cell surface proteins are also called "biomarkers" and have high affinity for their natural substrates or ligands.

Binding of radiolabeled or fluorescent ligands to the overexpressed cell surface proteins helps detection of diseased cells and distinguishes them from normal and healthy tissues. On the basis of this principle, several new methods were discovered for molecular imaging applications. Among those methods, magnetic resonance spectroscopic imaging (MRSI); radionuclear imaging such as single photon emission CT (SPECT), and positron emission tomography (PET); and optical imaging techniques are the most commonly described modalities for detection of malignancy.[1-3] Separately or in combination with conventional tools, these techniques are employed to understand the cellular processes responsible for the onset and progression of the diseases and for the evaluation of new cancer imaging agents and drug candidates.

A recent study conducted by the American Cancer Society states that worldwide there were 729 000 new cases of cancer in 2018. It is now estimated that 27 million people will be diagnosed for cancer by 2030 resulting in 17 million deaths every year.[4] This is partially attributed to the use of tobacco and high-fat diets, but a lack of early detection and diagnostic methods is an indirect cause for cancer-related mortality and morbidity. Among all the cancers, prostate cancer (PCa) is the second leading cause of death, next only to lung cancer among men in the United States, accounting for 30 000 deaths per year. Moreover, approximately 161 360 patients were annually diagnosed to suffer from PCa in the United States and 1.1 million men worldwide,[5] making it a lethal disease with a significant health burden on the society. The estimated health care cost for treatment and maintenance of newly diagnosed PCa patients is quite expensive and amounts to $8 to $10 billion per annum in the United States.[6] Furthermore, the quality of life of a newly diagnosed PCa patient is immensely affected because of psychological and emotional challenges. This is because the quality of life generally depends on the differences in the treatment modalities employed and stages of cancer. Whereas surgical treatment causes urinary incontinence, erectile dysfunction, and polyuria, radiation therapy results in momentary urinary obstruction, irritation of bowel, fecal incontinence, and painful hemorrhoids. Also, PCa in its advanced stages tends to metastasize to distant organs and bones, which affects the patient's life significantly due to bone erosion, cognitive decline, muscle wasting, and osteoporosis side effects.[7] Therefore, accurate initial diagnosis to determine the stage of disease remains to be a major challenge in the PCa treatment.

Considerable efforts have been directed to critically analyze and summarize all the research activities in the field of PCa diagnosis for the past several decades. Reviews detailing the importance and discovery of new molecular biomarkers[8] for prognosis and the currently used diagnostics and therapeutics[9,10] for PCa have been published. In 2018, refined advances in prostate-specific membrane antigen (PSMA)-targeted PET/CT imaging techniques[11-15] using various positron emission radioisotopes for early detection of PCa, management of metastatic castration-resistant prostate cancer (mCRPC), and their applications in detection of recurrent disease by guided biopsy and surgery[16] were published. There are also recent reports that exclusively cover clinical translation of PSMA-targeted ^{68}Ga and ^{177}Lu radioisotopes for detection and therapy of PCa in humans.[17-19] However, a comprehensive analysis exhaustively describing various diagnostic methodologies using targeted molecular imaging techniques is yet to be compiled. The objective of this report is to fulfill this gap by providing a critical analysis and detailed comparison of molecular imaging technologies based on different PSMA targeting motifs generated for the past several decades till today for detection of prostate malignancy in our laboratory as well as other research groups across the world.

2 | CONVENTIONAL DIAGNOSTIC METHODS

Current diagnosis of PCa is most often carried out through digital rectal exam (DRE), measurement of prostate-specific antigen (PSA) levels in serum, needle biopsy of disease suspected tissue using transrectal ultrasound (TRUS) technique.[20] However, during examination by DRE or prostate biopsy, high physical discomfort is reported by the patients making it a less preferable diagnostic method.[21] Another disadvantage of DRE is that it can only detect the PCa in its more advanced stages as the small grade tumors escape the attention when the disease is in the early stage of manifestation.[22] Although the Food and Drug Administration (FDA) approved PSA blood test is the most commonly employed screening test to detect prostate malignancy in the United States, its elevation in the serum level during benign prostatic hyperplasia (BPH), prostatitis, prostatic infarction, and urinary tract infections results in high false-positive tests and low specificity rates creating a controversy on its reliability.[23] Further, a decline of PSA level in the blood while undergoing treatment for BPH or alopecia necessitates the requirement of additional tools to predict the accuracy of the disease detection.[24] In addition, proton magnetic resonance spectroscopy (MRS) in combination with MRI provides accurate localization of the disease in certain regions of the prostate organ such as apex when compared with blind sextant biopsy.[25,26] Other than the aforementioned techniques, pelvic lymph node dissection (PLND) is the most commonly employed diagnostic method when the organ confined PCa spreads to lymphatic tissues. However, this method is invasive, expensive, and associated with high rate of sickness.[27] Under such circumstances, noninvasive CT and MRI are preferred methods for staging the lymph nodal metastatic disease because of its higher specificity. But a recent statistical analysis of the literature data collected over two decades reveals that these methods cannot accurately detect and distinguish lymph node metastasis from localized PCa.[28] Therefore, more sensitive and specific methods of detection are required to assess the primary and metastatic stages of disease to considerably reduce cancer-related morbidity and mortality in the world.

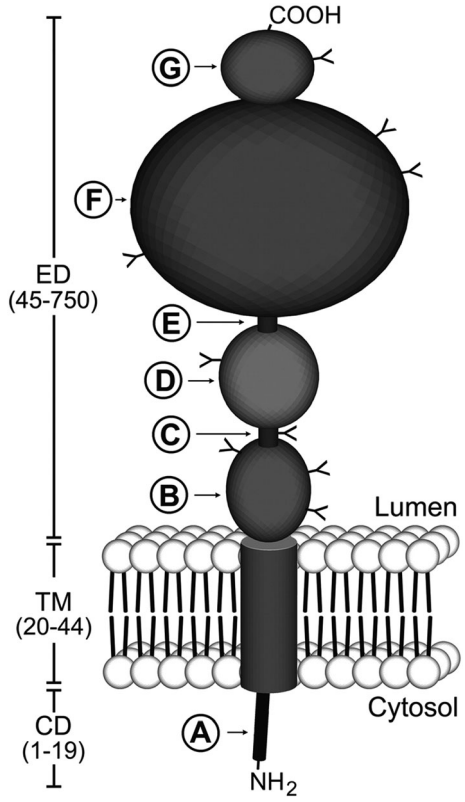

FIGURE 1 Schematic diagram of prostate-specific membrane antigen (PSMA) structure. PSMA is a type II transmembrane protein with a short NH_2-terminal cytoplasmic domain (CD), a hydrophobic transmembrane region (TM), and a large extracellular domain (ED). The CD contains an endocytic targeting motif and filamin A (FLNa) binding site (A). The large ED is highly glycosylated with nine predicted N-glycosylation sites (Y). The ED contains two domains of unknown function that span amino acid residues 44-150 (B) and 151-274 (D), proline- and glycine-rich regions that span amino acid residues 145-172 and 249-273, respectively (C and E), a catalytic domain that spans amino acid residues 274-587 (F), and a final domain of unknown function (amino acids 587-750) to which a helical dimerization domain (amino acids 601-750) is localized (G). Reproduced with permission from Rajasekaran et al[32]

3 | PROSTATE CANCER BIOMARKER

In order to overcome the constraints involved in the existing diagnostic methods for PCa, untiring efforts by various researchers across the world have led to the discovery of a special cancer biomarker called prostate-specific membrane antigen (PSMA) that is highly overexpressed on PCa cells.[29,30] PSMA is one of the most extensively studied biomarker among the 91 known PCa biomarkers, which are in one way or other related to the origin of PCa, its progression, and recurrence after primary treatment.[31] PSMA belongs to a family of type II membrane bound glycoproteins[32] overexpressed on the cell surface of most of the PCa cells (Figure 1). It is not a secreted protein in quite contrast to the other two prostate proteins such as PSA and prostatic acid phosphatase (PAP).[33] Crystal structure analysis of the PSMA's external peptide chain,[34] which consists of 44 to 750 amino residues and two zinc atoms, revealed deep insight into the binding pockets of the ligands or inhibitors, catalytic sites, and substrate hydrolysis mechanism of this enzyme (Figure 2). This can provide rationale for molecular designing of new PSMA targeting motifs that can be used for diagnosis and treatment of PCa and neurological diseases.[35] PSMA is also called as glutamate carboxypeptidase II or folate hydrolase due to its enzymatic ability to cleave terminal glutamate moiety from the neurodipeptide, N-acetyl-aspartyl-glutamate (NAAG), and γ-linked polyglutamates.[36] Even though physiological function of the PSMA remains unclear,[37] its overexpression during the onset of PCa was confirmed unequivocally by performing immunohistochemical staining on several normal and malignant tissues.

Also, the expression level of the PSMA markedly increases in the advance stages of the cancer[36,38-40] especially in poorly differentiated

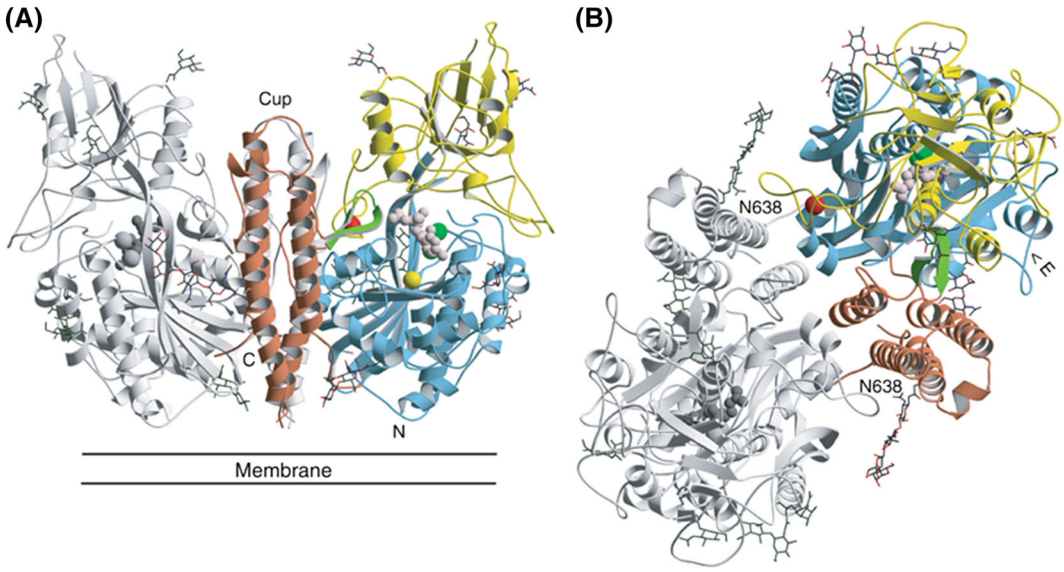

FIGURE 2 A, Structure of GCPII (A, B). Three-dimensional structure of the dimer. One subunit is shown in gray, while the other is colored according to organization into domains. Domain I (light blue), domain II (yellow), and domain III (brown). The dinuclear zinc cluster at the active site is indicated by dark green spheres, the Ca^{2+} ion near the monomer-monomer interface by a red sphere, and the Cl^- ion by a yellow sphere. The GPI-18431 inhibitor is shown as small beige balls. The "glutarate sensor" (the β15/β16 hairpin) is shown in light green. The seven carbohydrate side chains located in the electron density maps are indicated. The position of the structure relative to the membrane is shown in (A). B, Provides a view into the "cup" of the dimeric enzyme. The entrance to the catalytic site is indicated ("E"). Reproduced with permission from Mesters et al[34]

hormone refractory PCa[41,42] and metastatic PCa of lymph nodes, bone, rectum, and lung tissues.[43-45] The PSMA expression in androgen-independent metastatic tumor is especially considered crucial because almost all the types of PCa eventually becomes hormone-independent and resistant for treatment with the known therapeutic agents. At this stage, no cure is known for the disease affecting the patient's life irreversibly. PSMA's expression is originally thought to be confined to the prostate organ, but later studies have demonstrated that it is also expressed in several benign tissues such as proximal renal tubules, duodenum, colon,[37] and brain[23,46] albeit many times lower when compared with tumor tissues.[36] At last, recent findings disclose that the PSMA is also expressed in the endothelial cells of tumor-associated neovasculature of several nonprostatic solid malignancies but not in the normal or healthy blood vessels. This condition is utilized to deliver diagnostic or therapeutic agents during nonsmall cell lung cancer, colorectal carcinoma, and glioblastoma other than the PCa.[38,47] Collectively, PSMA's unique characteristics and its expression of a million receptors per cancer cell[48] renders it as the most suitable biomarker for diagnosis of primary and metastatic PCa by PSMA-targeted molecular imaging agents.

PSMA-targeted molecular or functional imaging agents that are currently employed for the diagnosis, staging, and prognosis of PCa can be broadly classified into two categories: radionuclear and optical imaging agents. They can be derived from PSMA-specific antibodies,[45,49-81] small molecular weight ligands,[82-122] targeted nanoparticles,[123] peptides,[124,125] peptide derivatives,[126] aptamers,[127-136] and engineered antibodies.[137,138]

3.1 | Radionuclear imaging agents

Approximately, 80% of all the radiopharmaceuticals used in the nuclear medicine technology are ^{99m}Tc-labeled compounds.[49] The 6 hours half-life, 140 keV decay photons and the ease of production of millicurie amounts of ^{99m}Tc from a generator, allows a radiochemist to quickly carry out the radiopharmaceutical preparation and to collect useful images with high spatial resolution in short time. The desirable properties of ^{99m}Tc made it as the most commonly used radionuclide in diagnostic nuclear medicine technology followed by ^{111}In ($t_{1/2}$ = 2.83 days). Whereas short-lived positron emitting nuclides used in clinical PET studies (^{18}F [$t_{1/2}$ = 109.8 minutes], ^{68}Ga [$t_{1/2}$ = 67.7 minutes], ^{11}C [$t_{1/2}$ = 20.4 minutes], ^{13}N [$t_{1/2}$ = 9.96 minutes], and ^{15}O [$t_{1/2}$ = 2.04 minutes]) have only restricted applications due to their rapid decay and the tedious nature of their production. Nevertheless, ^{18}F and ^{68}Ga isotopes are increasingly employed for acquiring high-resolution PET images. ^{68}Ga has attracted more attention recently because of its ease of production from ^{68}Ge/^{68}Ga generator unlike ^{18}F radioisotope that requires an in-house cyclotron facility.

3.1.1 | Monoclonal antibody

SPECT and PET radioisotopes–labeled monoclonal antibodies

The first monoclonal antibody (mAb) specific to PSMA, 7E11-C5.3, also known as CYT 356, was developed in the late 1980s using hybridization technique from murine IgG1. The radioactive version

of the antibody, 7E11-C5.3-GYK-DTPA-^{111}In conjugate, was shown to localize in the xenograft mouse model of PCa.[45] Since then, mAb has spurred interest in the development of new imaging agents for the detection of human PCa and had become a new diagnostic tool in the field of prostate oncology. Initial pharmacokinetics studies demonstrated that the mAb immunoconjugate CYT-356 specifically localized in LNCaP cells with a tumor to blood ratio of 3:1. Further, clinical trials of PCa patients with ^{111}In-CYT-356 conjugate by scintigraphy technique was promising and shown to detect both localized as well as metastatic PCa's with high specificity where conventional imaging modalities failed to detect any distant metastatic or soft-tissue lesions.[51] Because of this success, it was approved by the FDA for noninvasive imaging of metastatic PCa patients under the commercial name "ProstaScint" (Cytogen Corporation, Princeton, NJ). It is also called as ^{111}In-labeled capromab pendetide or "immunescan." The antibody conjugate binds to the intracellular domain (N-terminus) of the PSMA and therefore believed to detect only the necrotic or membrane ruptured cells of the prostate tumor.[52] ^{111}In-capromab pendetide detects primary and metastatic diseases in patients in whom pelvic lymphadenectomy is planned before radical prostatectomy.[53,54] Further, a phase II clinical trial of ProstaScint detects the sites of occult recurrence,[55,56] bone metastases, pelvic node recurrence, and the extent of metastatic spread in the men with hormone refractory disease.[57] However, the extent of primary tumor or capsular invasion cannot be confirmed using this mAb, and the interpretation of the scan result was highly difficult due to poor tumor-to-background ratio and lack of anatomical references.[46] According to another study, the ^{111}In-CYT-356 conjugate was shown to have better prostate:muscle ratio (greater than three) in the prostate bed during the recording of SPECT pelvic images. This study was shown to correlate well with the high incidence of residual PCa following prostate biopsy.[58-60] The ProstaScint scan even detected far distant metastasis of the PCa such as to the lung in a patient who does not show any evidence of the recurrent disease 11 years after prostatectomy.[61] Recently, to simplify the interpretation of ProstaScint scan, hybridization of SPECT with CT and MRI was performed to provide three-dimensional (3-D) hybrid images of the tumor that has been metastasized to prostate capsular region and seminal vesicles with higher accuracy. The problems associated with the two-dimensional (2-D) SPECT scans are inherent in most of the antibody-based imaging methods due to the special characteristics of tumor blood vessels. Tumor blood vessels are usually leaky, which is favorable in the sense that it enables antibodies to easily reach cancerous cells from the blood stream. But due to the heterogeneity of the tumor vessel leakiness, antibody distribution is not always uniform thereby decreasing the scan accuracy. The situation is further aggravated due to the accumulation of ProstaScint at the inflammatory sites of the prostate tissues that often coexists with the tumor of prostate gland. All these disadvantages would be overcome by suppressing inflammatory site uptake using 3-D hybridization methods. The 3-D technology is a useful addition tool for oncologists who would have to otherwise undertake special training to interpret cumbersome 2-D SPECT images.[62]

A typical ^{111}In-capromab scan using planar or SPECT technique takes up to 3 or 5 days postinjection because of slow uptake of the antibody by the diseased tissues. Moreover, considerable bone marrow uptake of ^{111}In-capromab conjugate will play a crucial role in the resolution of the scan because of the presence of bony structures in the pelvic region and location of the prostate gland. Additionally, the longer imaging time required during ^{111}In-capromab scan allows the gut excreted portion of the antibody to accumulate in the intestine and colon tissues. This warrants the use of laxatives by patients to avoid considerable background distraction in signals prior to imaging. Therefore, a new radioimmunoconjugate, ^{99m}Tc-7E11-C5.3, also called as CYT-351, was prepared and demonstrated to show considerable advantages over ProstaScint scan. The merits are due to attractive features of ^{99m}Tc radioisotope that are short half-life ($t_{1/2}$ = 6.02 hours), low radiation dose, affordable cost, minimal bone marrow uptake, and short scan session thereby avoiding the usage of laxatives.[63,64] CYT-351 is derived from bis (thiosemicarbazone) technetium chelating ligand, CYT-395, having a free hydrazide side chain available for conjugation with mAb (7E11-C5.3) sugar moiety. Radioimmunoscintigraphy scan using CYT-351 conjugate in prostate patients proved to be a sensitive and specific method for staging localized tumor, extraprostatic spread, lymphatic, and nodal metastasis.[65]

It is pertinent to weigh the potential benefits of ProstaScint against the adverse effects it causes in the biological systems before glorifying its usage as an affordable diagnostic tool for PCa detection. The most common side effects of this antibody agent are hypotensions and hypertensions, elevation in bilirubin levels and liver enzymes following its administration. Since the mAb is derived from the mouse, it is considered as a foreign body protein, and patients may produce human anti-mouse antibody (HAMA) reaction. Also, its intracellular binding site raises a doubt about its binding to viable PCa cells. Further, metastatic bone marrow disease is elusive to ProstaScint scans in most of the cases resulting in false negatives due to the absence of any necrotic or dead cells in bones.[42] In order to overcome the problems associated with ProstaScint, another anti-PSMA mAb, J591, that binds with high (1 nM) affinity to the extracellular domain of PSMA was developed and studied clinically.[66] Unlike the human immunoreactive 7E11-C5.3 antibody, the murine antibody J591 was immunosuppressed by genetic engineering of human immunoglobulin G1 (IgG1) protein. This modification of mAb retains specific affinity to PSMA and at the same time renders it as a "nonforeign" to human immune cells.[67] Further, J591 undergoes PSMA mediated internalization once it binds to the viable PCa cells.[68] These properties allowed radiolabeled J591 antibody to enter two phase I clinical trials in patients with advanced hormone refractory cancer[69,70] and solid tumors[71] with acceptable toxicity.

PSMA is also expressed in the neovasculature of most of the solid tumors and several other adenocarcinoma's such as lung, colon, breast, renal, transitional cells, and pancreas. Fortunately, PSMA's absence in the vasculature of normal tissues created an opportunity to image malignant blood vessels. In this context, radiolabeled-immuno conjugate ^{111}In-DOTA-hu J591 was evaluated in phase I clinical trial and shown to be a useful neovascular imaging agent for patients with

nonprostate solid tumors.[72] This opened-up a new alternative approach in imaging PCa and recently, another mAb, 3/A12 mAb, produced by hybridization of SP2-0 myeloma cells and spleen cells from a BALB/c mouse was demonstrated to show high binding affinity (2 nM) to the extracellular domain of PSMA in LNCap cells.[73] The antibody, 3/A12 mAb, was radiolabeled with PET nuclide ^{64}Cu ($t_{1/2}$ = 12.7 hours) through a conjugating moiety, DOTA, without compromising the binding affinity to PSMA. Further, using small animal PET imaging technique, ^{64}Cu-DOTA-3/A12 mAb was assessed for in vivo uptake in severe combined immunodeficiency (SCID) mouse bearing PSMA positive C4-2 tumor xenografts. Favorably, biodistribution studies show maximum uptake of 35% ID/g of tissue at 48 hours postinjection, but higher uptake of 16% ID/g in blood limited its entry to clinic in an unmodified form.[74]

Other than the PSMA biomarkers, prostate tumors also express high levels of specific tumor-associated carbohydrate antigens (TACAs), which can also be of valuable tools for in vivo detection of PCa. In this direction, an mAb H6-11 labeled with ^{125}I was evaluated using a commercial array of human PCa and normal tissue samples (n = 49) in which H6-11 detected 95% of the prostate adenocarcinomas. These adenocarcinomas overexpress a glycoprotein called β-N-acetylglucosaminidase (OGlcNAc) that can be recognized by H6-11 antibody through antibody-antigen reaction. Later, in vivo imaging studies were carried out in PC-3 tumor-bearing mice using NIR fluorescent dye-labeled H6-11 and ^{89}Zr-labeled H6-11 antibody in micro-PET modality. During these in vivo studies, the labeled probes accumulated in considerable amount in the liver. However, the liver showed significant clearance after 120 hours postinjection with the clear evidence of retention in tumors. These studies suggest that the mAb H6-11 conjugated agents are potential tools to detect PCa in vitro and in vivo.[75]

Before making any decision on the selection of antibodies employed for diagnosis of PCa, it is equally important to understand the resolution of radionuclide imaging techniques such as SPECT and PET to acquire precise and sharp images of the diseased tissues. The resolution of each radionuclear technique depends both on the affinity of the homing moiety (antibody) to the receptor as well as on the energy and mode of generation of the decay photons from the respective radioisotopes by a nuclear event.

In the case of SPECT, a γ-ray is emitted from the decaying radioisotope accumulated within the targeted tissues, whereas in the case of PET, two annihilation photons are generated when a positron emitted by the decaying PET radioisotope collides with an atomic electron in the annihilation event. PET has superior spatial resolution because of the emission of two collinear photons during each annihilation event, whereas in SPECT, only single γ-ray photon is generated for each nuclear de-excitation event.[76] Thus, greater affinity of the antibody to the receptor as well as collimated photons produced during PET process results in acquiring higher resolution images compared with SPECT.

The section above describes in detail the binding affinity, targeted epitope of PSMA by the different mAb, and the type of radionuclear techniques used for detection of PCa. From the above discussion, it is observed that 7E11-C5.3 antibody (CYT-351), chelated to SPECT radioisotope such as ^{99m}Tc, for detection of PCa is unreliable as it binds only to the necrotic cells or intracellular domain of the PSMA protein. Moreover, several modifications of CYT-351 were also found to be not very promising. But the J591 antibody version binds to the PSMA's extracellular domain with high affinity of 1 nM concentration. Its internalization on binding to the PCa cells and nonsusceptibility to attack by the immune system are some of the excellent properties, which makes it a more favorable antibody for detection of PCa. Even though 3/A12 antibody (2 nM) also showed comparable binding with PSMA expressed on LNCaP cells, making it a viable candidate for ^{64}Cu PET imaging, but its high accumulation in blood during the scan limits its applications for clinical success. Also, mAb, H6-11, has 60 times lower affinity (61.7 nM) when compared with J591 antibody. Moreover, the NIR and radioisotope-labeled versions of H6-11 showed high retention in liver for several days, rendering it as a less suitable diagnostic tool for in vivo tumor detection.

In conclusion, among all the monoclonal antibodies, J591, has shown the most promising results in terms of high binding affinity, less background interference and reliability to detect live PCa cells both in vitro as well as in vivo, justifying its success in the clinical trials.

Radiolabeled engineered monoclonal antibodies

Although radiolabeled mAb's are promising for PSMA-targeted imaging and therapy, there have been limited successes because of their long circulation half-life, poor tumor penetration ability,[77] high cost of production, and sophisticated handling techniques.[78,79] Partially, these drawbacks were addressed by using engineered mAb fragments of J591 for the detection and staging of PSMA positive prostate tumors by PET technique where it has been shown that ^{89}Zr-Minibody and ^{89}Zr-Cys-Diabody undergo rapid background clearance, essentially establishing these scFv-based antibody fragments as faster alternatives to the whole mAb.[80]

Because of the limitations associated with PSMA-targeted mAb imaging agents, variety of low molecular weight PSMA inhibitors have been designed, synthesized, radiolabeled, and used to image human PCa xenografts derived from LNCaP and PC-3 cell lines in mouse models. Deep penetration of small molecule ligands into tumor tissues including solid tumors improves signal to noise ratio. In addition, small molecule ligands have better pharmacokinetic profile—rapid biodistribution and rapid clearance—compared with high molecular weight antibodies making even smaller lesions easily visible. Lastly, small molecule ligands are labeled with various radionuclides such as ^{177}Lu, ^{125}I, ^{124}I, ^{123}I, ^{111}In, ^{99m}Tc, ^{68}Ga, ^{18}F, and ^{11}C in ease compared with mAb without considerable degradation.[81]

3.1.2 | Small molecule ligands for targeting PSMA

Phosphorus-derived ligands

An inhibitor of PSMA or NAALADase activity with an affinity of 9 nM called glycosylphosphatidylinositol (GPI) molecule was identified long ago as a potential candidate for small molecule imaging ligand. However, endogenous ligands such as phosphate ions present in the serum

compete with monomeric GPI ligand limiting its use for in vivo diagnostic applications of PCa. Therefore, to out-compete endogenous competitors, three molecules of GPI were attached to a rigid adamantane framework with free amino functionality to link technetium chelating moiety, MAS_3 (S-acetylmercaptoacetyltriserine). Using solid-phase ^{99m}Tc preloading strategy, ^{99m}Tc was attached to this chelation moiety separately and further transformed to an activated N-hydroxysuccinmide ester (NHS), ^{99m}Tc-MAS_3-NHS. The NHS ester intermediate was then conjugated to adamantine-trimerized GPI with free amino group to provide ^{99m}Tc-MAS_3-GPI_3 nuclear imaging agent. This technetium conjugate was demonstrated to have a high affinity of 3 nM concentration for PSMA positive LNCaP cells during in vitro study rendering it as a valuable diagnostic agent for clinical use.[82]

Urea hetero/monodimer ligands

a. Lys-NHCONH-Glu ligand with tridentate chelating moiety

After the preliminary use of phosphorus-derived molecule (GPI), urea-based PSMA inhibitor (Lys-NHCONH-Glu) with variable linker length was described.[83] In this study, a series of urea-based inhibitors, containing tridentate moiety for chelating ^{99m}Tc, with high to moderate affinity for PSMA positive PC3 PIP tumors have been demonstrated using SPECT-CT imaging technique. One of the compounds with an aminooctanoic acid spacer between the urea-lysine ligand and chelation moiety showed best results in terms of selective tumor uptake (7.9% ID/g tissue) at 30 minutes postinjection, high target to nontarget ratio (44:1) at 2 hours postinjection, and rapid clearance from normal tissues, making it as a potential clinical candidate to study PCa patients.

b. Glu-NHCONH-Glu or DUPA ligands with chelating moiety

Computational molecular docking study to find optimal targeting ligand for PSMA using high-resolution crystal structure of the ectodomain of NAALADase in complex with one of its high affinity inhibitors (GPI-18431) led to the discovery of another urea-based PSMA ligands called DUPA (2-[3-(1,3-dicarboxypropyl)ureido] pentanedioic acid).[84,85] DUPA is a symmetrical urea monodimer derived from L-glutamic amino acid. Theoretical calculations to fit the DUPA ligand into the crystal structure of PSMA enzyme revealed the requirement of electrostatic interactions of three of the carboxylic acids of DUPA with arginine and lysine amino acid residues of the peptide chain. Additionally, the oxygen atom of the urea functionality must directly coordinate with the zinc atoms present in the active site of the enzyme. The fourth free γ-carboxylic acid group will provide a handle for conjugation of chelating moiety via different peptidic spacers of varying length. Among the various conjugates examined to have better affinity for PSMA, optimal binding was found with a targeted conjugate containing two phenyl alanine residues between DUPA and chelating moiety. This ^{99m}Tc-DUPA-conjugate is now being tested at the Indiana University Medical School, USA, rendering it as the first ^{99m}Tc-chelated small molecule nuclear imaging agent to enter clinical trial (Figure 3).

A preliminary investigation of ^{99m}Tc-DUPA-conjugate in LNCaP-derived xenograft implanted on athymic nude mouse displayed 12.4% ID/g tumor uptake at 4 hours postinjection compared with only 7.9% ID/g tumor at 30 minutes postinjection reported for Lys-NHCONH-Glu–based PSMA inhibitors.[83] This difference in tumor uptake between ^{99m}Tc-DUPA and Lys-NHCONH-Glu–based radiolabeled conjugates might be attributed to the nature of spacers and their interaction with the binding pockets of PSMA in different manner. The higher uptake of ^{99m}Tc-DUPA-conjugate in tumor increases the signal to noise ratio and tumor retention time thereby providing greater contrast between cancer and nontargeted tissues.

c. Lys-NHCONH-Glu ligand with chelating moieties-DOTA, HBED-CC

Urea-based ligand, Lys-NHCONH-Glu, was also conjugated to a chelating agent, DOTA, through different spacers[86] to chelate radiometal ^{68}Ga (Figure 4) and employed for the identification of $PSMA^+$ tumors using small animal PET studies. During this study, it was demonstrated that ^{68}Ga-radiolabeled PSMA conjugates show high PCa tumor specificity (Figure 5) and found to be a favorable alternative to the traditional ^{18}F-radiolabeled cancer imaging agents since the former does not require an in-house cyclotron facility.

Following this first report, PSMA inhibitor Lys-NHCONH-Glu was also conjugated to another radiogallium chelator, HBED-CC, and in vivo studies were compared with the corresponding DOTA chelator. Compared with the DOTA conjugate, the ^{68}Ga-radiolabeled HBED-CC chelator has reduced nonspecific uptake and showed fast plasma and organ clearances with low liver accumulation and high

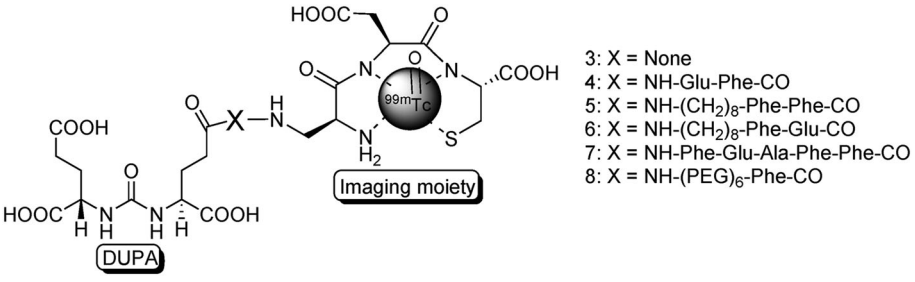

FIGURE 3 Structures of ^{99m}Tc-DUPA conjugated anti-PSMA radiotracers with various spacers, where X = peptide spacer and three letter code indicates different amino acids. Reprinted (adapted) with permission from Kularatne et al[84]

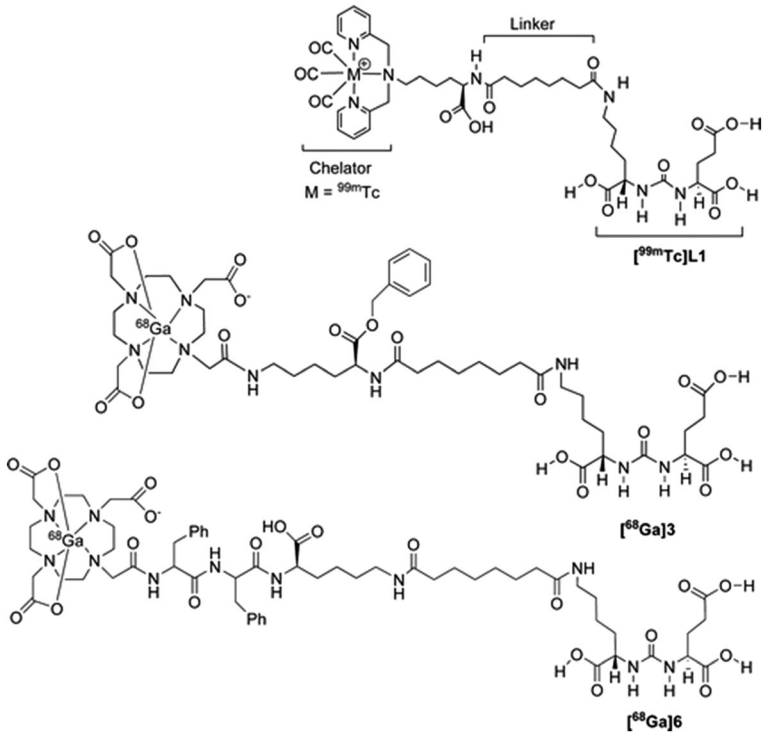

FIGURE 4 Urea-based PSMA conjugates [^{68}Ga]3 and [^{68}Ga]6 for small animal PET/CT applications. Reprinted (adapted) with permission from Banerjee et al[86]

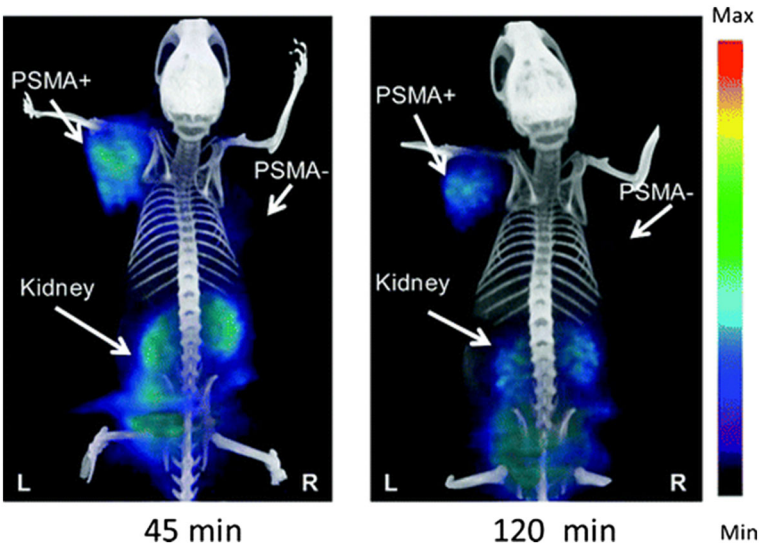

FIGURE 5 GE eXplore VISTA PET image (coregistered with the corresponding CT image) of a PSMA^{+} PIP and PSMA^{-} flu tumor-bearing mouse injected intravenously with 0.2 mCi (7.4 MBq) [^{68}Ga] Lys-NHCONH-Glu–based PSMA PET agent. Reproduced with permission from Banerjee et al[86]

specific uptake in PSMA expressing tumor.[87] This conjugate was shown to detect PCa relapses and metastasis with significantly improved contrast compared with traditional [^{18}F]FECH[88] and [^{18}F] FMCH PET/CT images[89] taken in several patients (Figure 6). Further, a biodistribution study of ^{68}Ga-radiolabeled HBED-CC conjugate in patients to detect PCa relapses and metastasis[90] showed better tumor to tissue ratio in addition to less understood high uptake in salivary glands and moderate accumulation in lacrimal glands, liver, spleen, and bowel tissues (Figure 7). Using the same PSMA inhibitor with a different spacer to improve pharmacokinetics, a first preclinical study and proof of concept in humans[91] was demonstrated later. The radiopharmaceutical was utilized for performing both imaging and therapy in patients with metastatic and castration-resistant PCas (Figure 8). This is the first PSMA-targeted theranostic agent called [^{68}Ga/^{177}Lu] PSMA-I&T probe. Later on, [^{111}In]PSMA-I&T was synthesized and evaluated as a complementary probe to [^{68}Ga/^{177}Lu]PSMA-I&T for radioguided resection of PSMA positive lesions using SPECT/CT technique and found to show improved background resolution.[92] Because

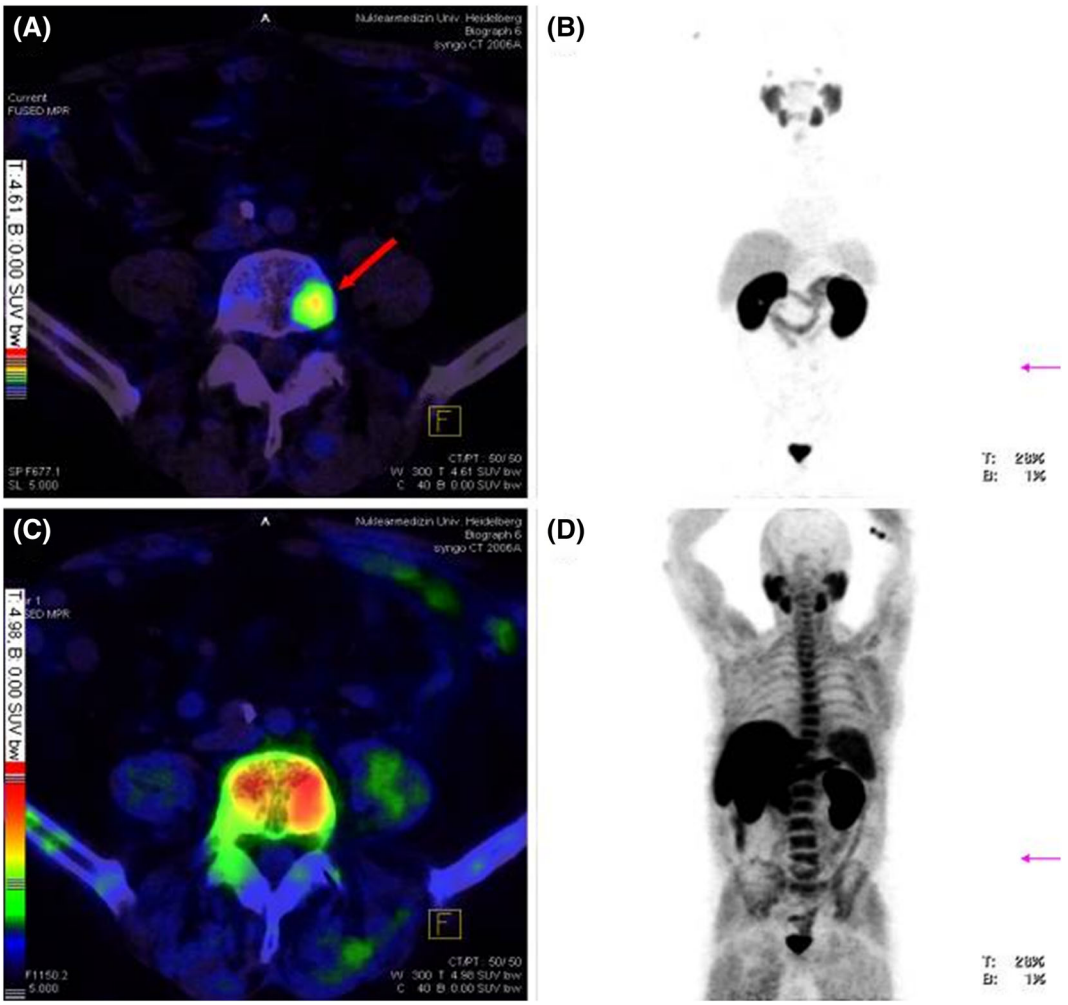

FIGURE 6 PET/CT imaging for detecting tumour metastasis in vertebral column of a PCa patient. (A) Fusion of ^{68}Ga-PSMA-PET and CT, red arrow points to a vertebral metastasis visible only via ^{68}Ga-PSMA PET/CT imaging as physiological high background makes vertebral metastasis difficult to detect by ^{18}F-fluoromethylcholine PET. (B) Maximum intensity projection (MIP) of ^{68}Ga-PSMA-PET. (C) Fusion of ^{18}F-fluoromethylcholine PET and CT, (D) MIP of ^{18}F-fluoromethylcholine PET. Reproduced with permission from Afshar-Oromieh et al[89]

each ^{177}Lu radioisotope decays by emitting a beta particle and a gamma ray, the probe is used for both therapeutic as well as imaging applications by scintigraphy and SPECT techniques. For optimum radioligand therapy (RLT), it is pertinent to calculate the absorbed dose in each organs, which was meticulously found out recently by using [^{177}Lu]DKFZ-PSMA-617 probe during the treatment of metastatic PCa.[93] From the ongoing discussions, it is clear that ^{68}Ga and ^{177}Lu radioisotopes also contribute immensely for imaging and therapeutic applications of PCa.

d. Lys-NHCONH-Glu ligand containing arylradiohalogens

As an extension of initial investigation[83] using urea-based PSMA inhibitor, Lys-NHCONH-Glu, the authors have also reported three new urea-based imaging agents by incorporation of radiohalogens such as ^{125}I and ^{18}F for SPECT and PET studies, respectively.[94] The imaging agents are called 2-[3-[1-carboxy-5-(4-[^{125}I]iodo-benzoylamino)-pentyl]-ureido]-pentanedioic acid, 2-(3-[1-carboxy-5-[(5-[^{125}I]iodo-pyridine-3-carbonyl)-amino]-pentyl]-ureido)-pentanedioic acid, and 2-[3-[1-carboxy-5-(4-[^{18}F]fluoro-benzoylamino)pentyl]-ureido]-pentanedioic acid. The ^{125}I-iodobenzoyl agent showed an uptake of 8.8% ID/g in PSMA^{+} PC-3 PIP tumor at 30 minutes postinjection similar to ^{125}I-iodo-pyridine (PSMA^{+} LNCaP tumor uptake) and ^{18}F-fluoro-benzoyl compounds at early time points. The images were recorded on SCID mice bearing tumors using a combination of SPECT/CT and PET/CT modalities. All these compounds demonstrate high target to nontarget tissue ratio making all of them for eventual clinical use.

Using Lys-NHCONH-Glu as a targeting moiety of PSMA, a series of halogen (F, Cl, Br, and I) substituted benzylamino and phenylamido nonradioactive analogs were evaluated in vitro in LNCaP cells. It was demonstrated that the nature and position of the halogen atoms in the aryl ring significantly affect the interactions of the probe with the binding pockets of PSMA. Overall, *para*-substituted iodine analogs were found to show best binding affinity to PSMA enzyme in nanomolar concentrations.[95] From the iodinated series two lead

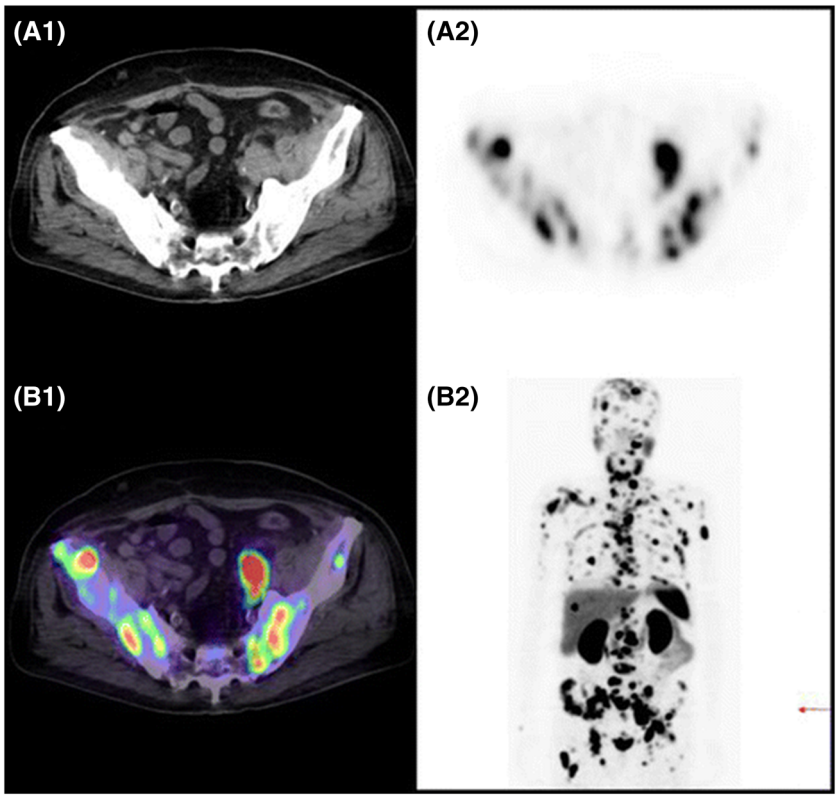

FIGURE 7 ^{68}Ga-Radiolabeled HBED-CC conjugate PET/CT imaging of lymph node and bone metastasis of prostate cancer in a patient. (A1) CT scan of a patient demonstrating disseminated lymph node and bone metastases of prostate cancer. (A2) ^{68}Ga-PSMA PET scan showing lymph node and bone metastases. (B1) Combined/merged image of ^{68}Ga-PSMA PET and CT scan of patient representative showing bone and lymph node metastases. (B2) Maximum intensity projection of image showing lymph node and bone metastases. Reproduced with permission from Afshar-Oromieh et al[90]

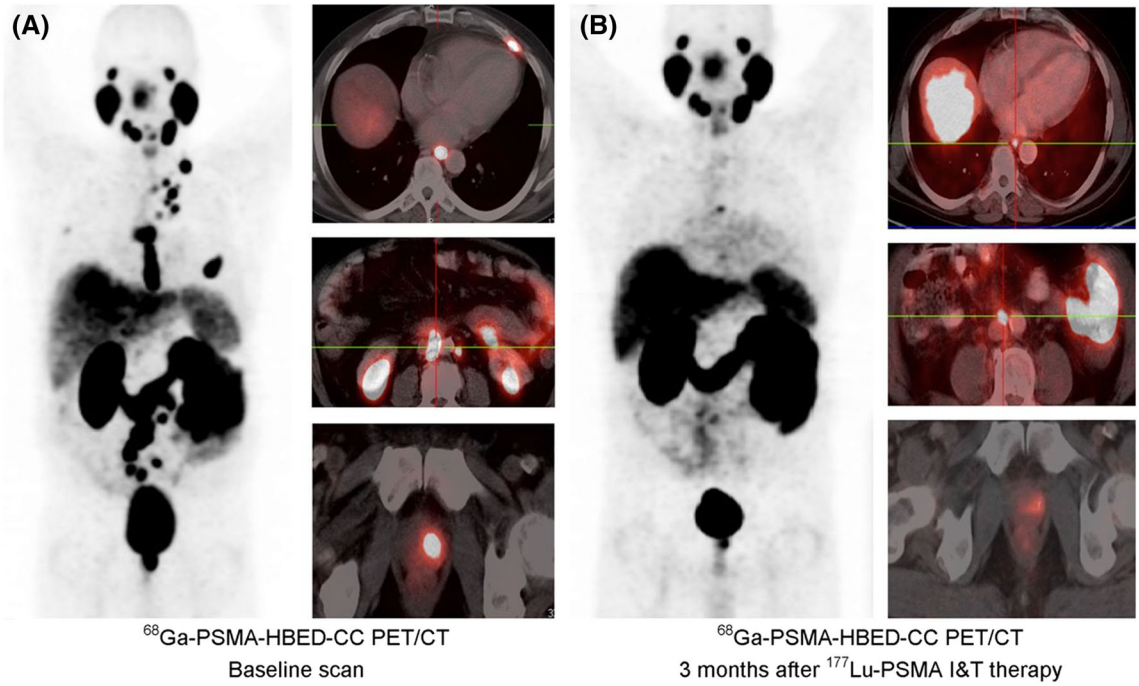

FIGURE 8 PET/CT in a PCa patient. A, Baseline PET/CT 65 min after intravenous administration of 176 MBq of ^{68}Ga-PSMA-HBED-CC. B, Follow-up scan with 180 MBq of ^{68}Ga-PSMA-HBED-CC (60 min after injection) performed 3 mo after ^{177}Lu-PSMA-I&T therapy (8.0 GBq). Reproduced with permission from Weineisen et al[91]

compounds, MIP-1072 [(*S*)-2-(3-((*S*)-1-carboxy-5-(4-iodobenzylamino) pentyl)ureido)pentanedioic acid] and MIP-1095 [*S*)-2-(3-((*S*)-1-carboxy-5-(3-(4-iodophenyl)ureido)pentyl)ureido)pentanedioic acid] were selected and radiolabeled with ^{123}I radioisotope.[96] Both [^{123}I] MIP-1072 and [^{123}I]MIP-1095 agents exhibit high affinity (3.8 and 0.81 nM) for PSMA on LNCaP cells during in vitro studies. Because of their high binding affinity to PSMA, [^{123}I]MIP-1072 and [^{123}I]MIP-1095 were taken further for in vivo imaging using SPECT/CT techniques on mouse bearing human LNCaP xenograft. Biodistribution studies on mouse showed high uptake of 17% ID/g tumor at 1 hour postinjection and 34% ID/g at 4 hours postinjection for [^{123}I]MIP-1072 and [^{123}I]MIP-1095 compounds, respectively, rendering them as potential clinical candidates for translation. Indeed, a phase I human clinical trial[97] has been already completed for these compounds in patients with metastatic PCa (Figure 9).

e. Glu-NHCONH-Cys/Tyr/Lys ligands containing radiocarbon or radioarylhalogens

Three radiolabeled urea derivatives (a) [^{11}C]DCMC, (K_i = 3.1 nM, N-[N-[(S)-1,3-dicarboxypropyl]carbamoyl]-S-[^{11}C]methyl-L-cysteine), (b) [^{125}I]DCIT, (K_i = 1.5 nM, N-[N-[(S)-1,3-dicarboxypropyl]carbamoyl]-S-3-[^{125}I]iodo-L-tyrosine), and (c) [^{18}F]DCFBC, (K_i = 13.9 nM, N-[N-[(S)-1,3-dicarboxypropyl]carbamoyl]-4-[^{18}F]fluorobenzyl-L-cysteine) were recently synthesized and evaluated for affinity to PSMA in SCID mouse bearing xenograft.[98-100] While [^{11}C]DCMC and [^{18}F]DCFBC imaging agents uptake in tumor-bearing mouse was characterized using small animal PET technique, [^{125}I]DCIT was evaluated using SPECT and gamma scintigraphic techniques. During these studies, [^{11}C]DCMC and [^{125}I]DCIT tracers showed an uptake of 8.7% ID/g tumor and 5.1% ID/g tumor, respectively, at 30 minutes postinjection, whereas the PSMA$^+$ PC-3 PIP tumor uptake for [^{18}F]DCFBC was found to be 6.2% ID/g. [^{18}F]DCFBC is considerably stable, and no significant defluorination was observed as evidenced by the minimal bone uptake. However, these radiopharmaceuticals show the highest uptake in the murine kidneys, but the fast renal clearance 2 hours postinjection relative to the targeted tissues makes them highly desirable for human clinical trials. In fact, a first-in-human clinical trial of the agent, [^{18}F]DCFBC, for the detection of metastatic PCa (Figure 10) and dose estimation study at various organs in comparison to a conventional radiopharmaceutical agent, ^{18}FDG, has been recently published.[101] Further, a second generation [^{18}F]-DCFPyL PSMA PET agent (Figure 11) was examined in preclinical studies on a murine model[102] followed by human clinical versions (Figure 12) to validate its selective accumulation in primary and metastatic PCa tissues.[103] During these studies, it was observed that [^{18}F]DCFPyL PET/CT agent was shown to detect more suspicious lesions in metastatic PCa patients than the conventional radioimaging techniques. The improved sensitivity of [^{18}F]DCFPyL agent is due to the fact that the urea derivative has a terminal glutamate moiety in the P1′ binding pocket of the PSMA protein enabling better affinity to the biomarker. In addition, the sensitivity of the PET scan has improved a lot to detect lesions in patients with metastatic clear cell renal cell carcinoma (ccRCC).[104]

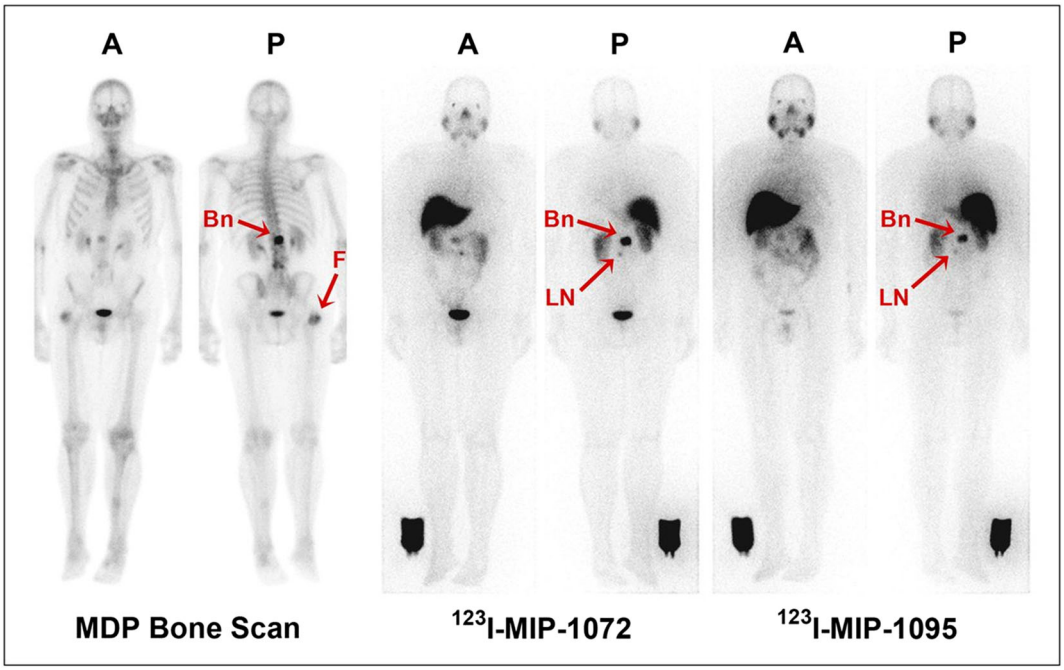

FIGURE 9 Representative anterior A, and posterior (P) whole-body planar images of patient with radiographically confirmed metastatic prostate cancer who received 740 MBq (20 mCi) of ^{99m}Tc-methylene diphosphonate (MDP) (left), followed by 123I-MIP-1072 (middle) and 123I-MIP-1095 (right) administered at 370 MBq (10 mCi). Depicted are images acquired at 4 h after injection. Arrows indicate detection of confirmed lesions in bone (Bn) of lumbar spine and uptake in suggestive 7-mm lymph node (LN). Image reference standard was placed next to right leg. Subject had previous hip replacement as demonstrated by uptake in head of right femur (F) only on bone scan. Reproduced with permission from Barrett et al[97]

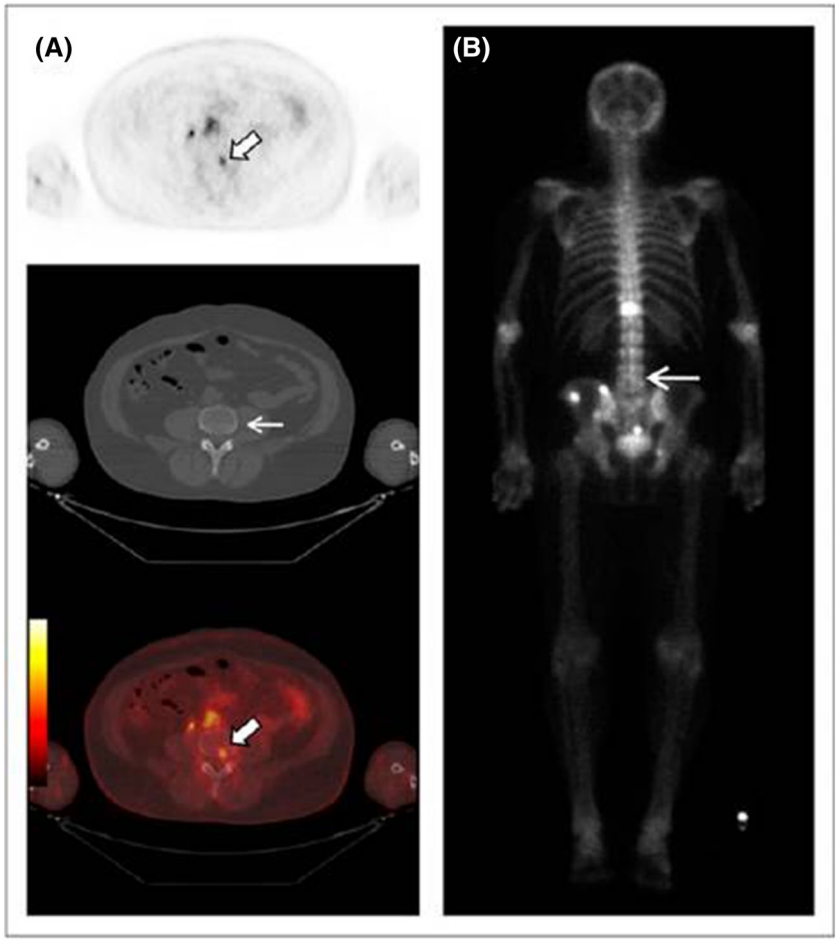

FIGURE 10 Focal ^{18}F-DCFBC PET uptake in L4 vertebral body on PET and fused PET/CT (thick arrows, A) with no correlative abnormality on CT (thin arrow, A) or bone scan (arrow, B). Reproduced with permission from original publication by Cho et al[101]

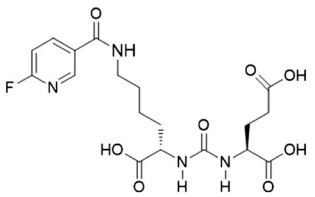

FIGURE 11 Chemical structure of [^{18}F]DCFPyL PET imaging agent. Reproduced with permission from Chen et al.[102]

In 2018, ^{18}F-PET imaging was combined with a fluorescent agent, trimethine cyanine dye, to produce color contrast for image-guided PCa management.[105] The ^{18}F radioisotope in the imaging agent provides for noninvasive nuclear imaging of PSMA expressing cancers in the prostate and lymph nodes, while the fluorescent dye allows for fluorescent guided surgery even after the decay of ^{18}F radioisotope. During surgery, this technology has a huge potential to improve surgeon's ability to better preserve nerve tissues, completely resect cancer, and detect lymph node micrometastases to extend lymphadenectomy or protect men from lymph node dissection.

(*S*)-2-[3-[(*R*)-1-Carboxy-2-mercaptoethyl]ureido-pentanedioic acid (Cys-NH-CO-NH-Glu) was also used to design novel PSMA targeting probes by nucleophilic conjugate addition between cysteine and maleimide-based radiohalogen fragment. By this strategy, [^{123}I] IGLCE was synthesized and shown to exhibit high affinity and specificity to PSMA positive tumors. The increase in binding affinity was attributed to the presence of an aromatic group in the radiopharmaceutical agent and a succinimide moiety to tether to the targeting moiety.[106]

f. Lys-NHCONH-Glu ligand labeled with ^{64}Cu radionuclide using macrocylic chelators

Very recently ^{64}Cu-labeled inhibitors[107] of PSMA based on lysine-glutamate urea scaffold with a variety of macrocyclic chelators, such as NOTA, PCTA, Oxo-DO3A, CB-TE2A, and DOTA, were investigated for in vivo PET imaging applications in SCID mouse harboring prostate tumor xenograft (Figure 13). During this study, it was shown that ^{64}Cu-labeled NOTA- and CB-TE2A-conjugated radiotracers exhibited favorable pharmacokinetics over the PCTA, oxo-DO3A, and DOTA conjugates. However, the superior tumor-to-background ratios provided by the CB-TE2A chelated [^{64}Cu] conjugate over NOTA-labeled conjugate proved it to be the most promising conjugate among all the other candidates tested in vivo. This could be due to higher in vivo stability and renal clearance of [^{64}Cu] CB-TE2A conjugate when compared with other chelating moieties (Figure 14).

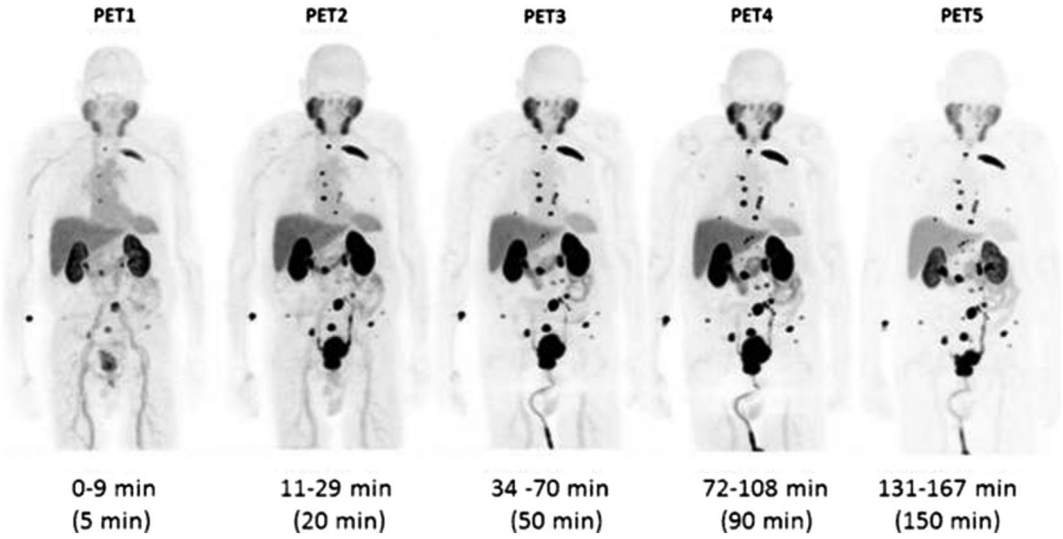

FIGURE 12 [^{18}F]-DCFPyL anti-PSMA maximum intensity projection (MIP) PET image sequence in a PCa patient. The patient demonstrated radiotracer binding in a large number of metastatic lesions involving multiple bones and lymph nodes. Reproduced with permission from Szabo et al[103]

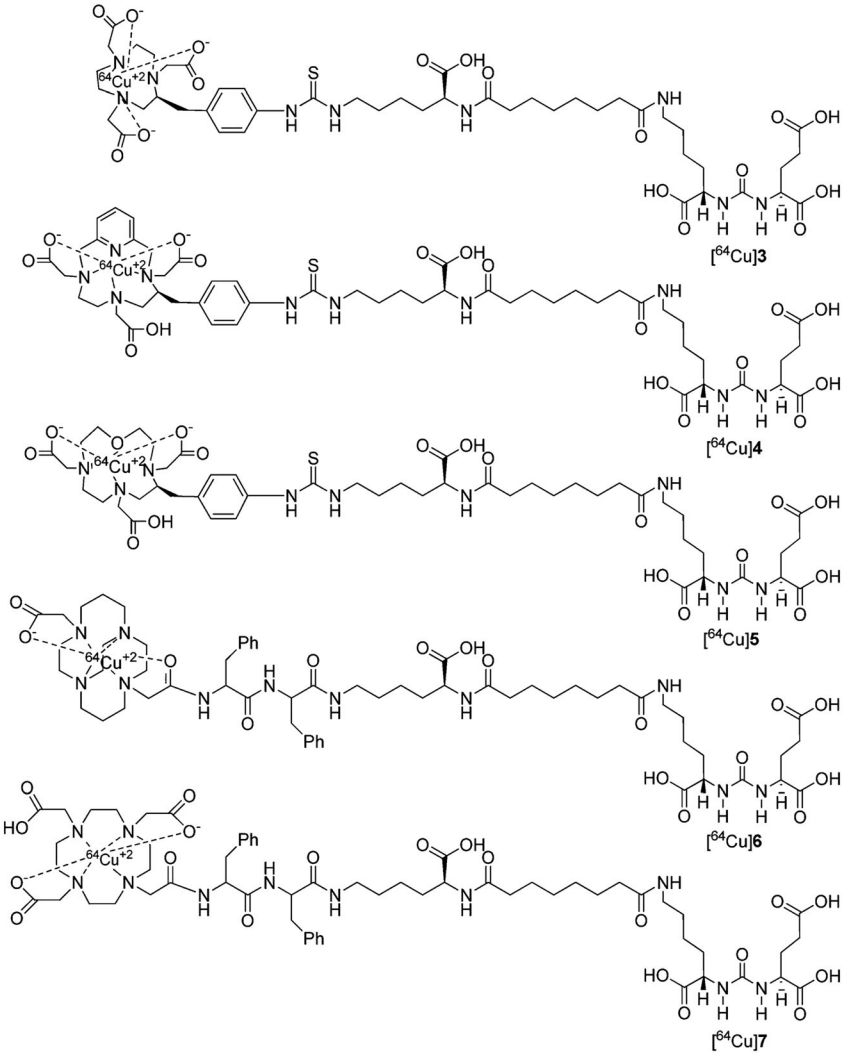

FIGURE 13 Structures of ^{64}Cu-labeled inhibitors of PSMA with NOTA, PCTA, Oxo-DO3A, CB-TE2A, and DOTA chelators for in vivo PET imaging applications. Reprinted (adapted) with permission from Banerjee et al[107]

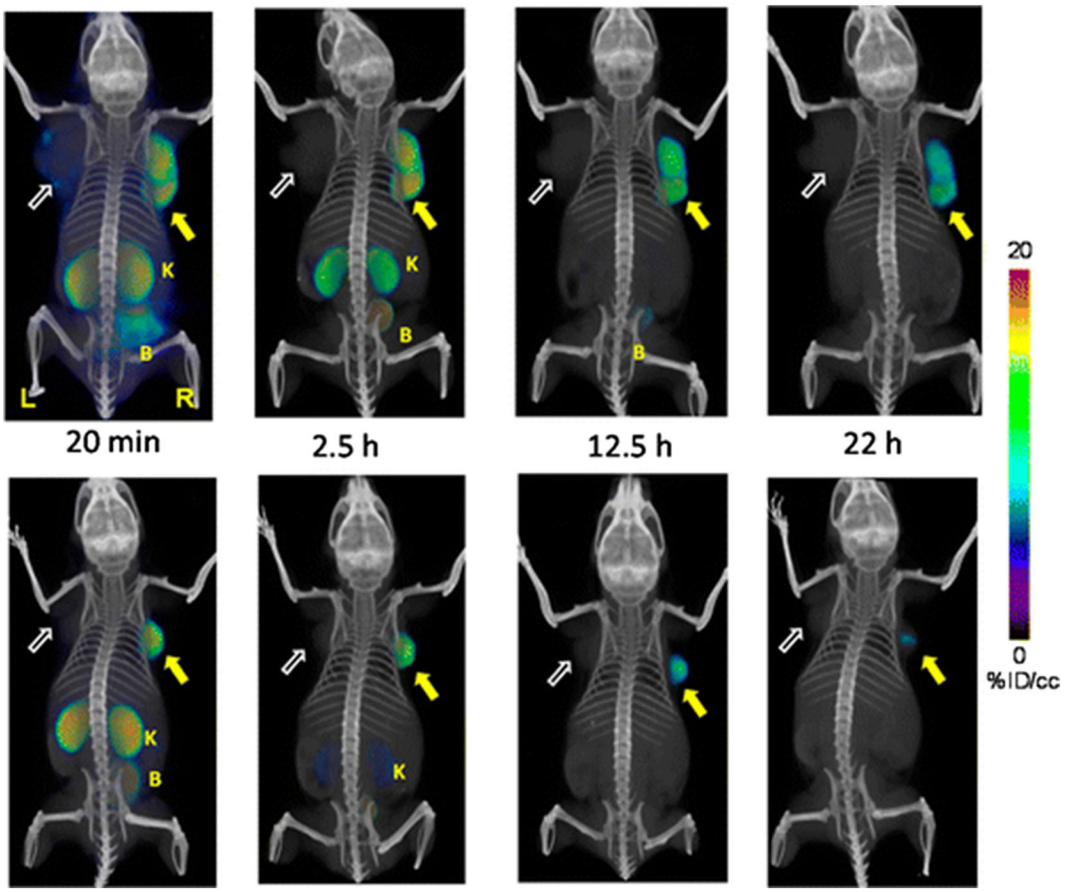

FIGURE 14 Whole body PET-CT imaging of PC3 PIP and PC3 flu tumor-bearing mice with [^{64}Cu]Lys-NHCONH-Glu inhibitor 6A as a building block (top row) and [^{64}Cu]Lys-NHCONH-Glu inhibitor 6B (bottom row) at 20 min, 2.5 h, 12 h, and 22 h postinjection. Abdominal radioactivity is primarily due to uptake within kidneys and bladder. PIP = PC3 PSMA+ PIP (solid arrow); flu = PC3 PSMA− flu (unfilled arrow); K = kidney; L = left; R = right, B = bladder. All images are decay-corrected and adjusted to the same maximum value. Reproduced with permission from Banerjee et al[107]

Phosphoramidate-derived ligands

Even though several urea ligands were reported for PSMA targeting, the literature is not replete with small molecules derived from phosphate ligand, which is a strong irreversible endogenous ligand for PSMA inhibition. One such class is a library of tetrahedral phosphoramidates that show pseudo-irreversible affinity for PSMA enzyme. The central core of the phosphate moiety is attached to glutamate residue and glutamate-serine dipeptide to give phosphoramidate-dipeptide ligand that show high binding affinity for inhibiting PSMA activity (IC_{50} = 14 nM). The free amino group of attached dipeptide is available for introducing radiolabeled tracer by conjugation chemistry. Following this concept, a ^{18}F-fluorobenzamido-phosphoramidate (IC_{50} = 0.68 nM) small molecule PSMA imaging agent was synthesized and evaluated for detection of prostate tumors.[108] Initial in vivo assessment of ^{18}F-phoshoramidate conjugate using PET in NCr nude mouse bearing LNCaP tumor show rapid localization of the tracer in the tumor with no uptake in the bones. Further, minimal uptake in the kidney and liver was observed when compared with urea-based imaging agents. Unfortunately, biodistribution study showed poor tumor uptake of only 1.24% ID/g at 2 hours postinjection necessitating the need for further structural modifications of this class of compounds.

Besides the abovementioned radiolabeled tracers, several new phosphate-based PSMA inhibitors such as phenalkyl,[109,110] steroidal phosphoramidate derivatives of glutamic acid,[111] and enantiomerically pure phenalkyl phosphonic acid derivatives[112] were also designed, based on molecular docking studies, chemically synthesized and demonstrated to have high affinity for PSMA enzyme. The radiolabeled analogs of such derivatives are yet to be realized for in vitro and in vivo imaging applications.

Therefore, it will not be an exaggeration to say that radiolabeled small molecules will have an edge over monoclonal antibodies by the next decade for detection, staging, and diagnosis of PCa due to their high rate of success in clinical trials. An ideal nuclear imaging agent should possess high tumor uptake, fast clearance from nonmalignant tissues, improved tumor penetration, functionality amenable for radiochemical synthesis, high radiochemical purity, long shelf life, and simple and short purification methods at the diagnostic center. Some of the small molecule ligands fulfill most of the above criteria and hence have found their entry into clinical trials. The functional imaging tools

such as SPECT and PET employed to image cancer patients are minimally invasive and provides accurate localization of tumor when used in conjunction with CT or MRI. However, the production of SPECT (^{99m}Tc) and PET radioisotopes (^{68}Ga, ^{18}F, and ^{11}C) may require either closely situated radionuclide generator or in-house cyclotron facilities as the radioisotopes decay rapidly due to short half-lives before being transported to far away medical diagnostic centers. For routine scans, these techniques may look quite expensive and unaffordable, but when calculated in terms of diagnostic value and quality of patient life, the merits of small molecule imaging agents outweigh the large cost factor involved in their preparation.

3.2 | Optical imaging agents

Despite their immense potential as diagnostic agents for cancer, one of the most common health concerns associated with the use of radionuclear cancer imaging agent is the exposure of patients to ionizing radiation while undergoing diagnosis for the detection of pathological diseased conditions. Even if shorter half-life radioisotopes are used for imaging patients, a residual exposure to high-energy gamma radiation or nuclear particles is unavoidable and may be led to undesirable side effects. Further, these nuclear imaging agents can only detect the site of disease but fail to marginalize its exact boundary. This is crucial in cancer disease treatment because most often minute metastatic lesions are missed during curative surgery and results in the recurrent disease in the later part of life.

3.2.1 | Intraoperative guided surgery for PCa

Cancer surgeries in general are performed without any intraoperative guidance leading to incomplete removal of tumors. There might be several nonguided techniques, which direct and improve current surgical procedures. However, other than intraoperative guided surgery, no method helps in complete resection of the tumor from the body. Nonguided techniques like the tactile approach provides suboptimal visualization during operation, which limits the surgeon's ability to accurately position surgical instruments during the procedure and heavily compromises the surgeon's ability to determine surgical endpoints. Till now, no method has been developed to visualize tumor lesions and tissues to an extent defined by intraoperative guided surgery. Therefore, more sensitive nonradiation imaging methods than the functional methods such as SPECT, PET, CT, and MRI are required for onsite guidance of surgery.

3.2.2 | Fluorescent dyes for optical imaging of cancer

Fluorescein dyes have been used since 1948 for intraoperative image guidance and resection of brain tumors. This technology called intraoperative photodiagnosis (PDD) has been recently revived with the advancement of optics and fluorescent dye chemistry.[113] More recently longer wavelength dyes or near-infrared (NIR) dyes (700-900 nm) have been utilized for in vivo imaging[114] and specifically for intraoperative image-guided PCa surgery.[115] Most of the living tissues show low auto fluorescence in the NIR region, and therefore, application of PSMA-targeted NIR dyes to image PCa patients may become an important tool in the arsenal of imaging agents.

Phosphorous-based fluorescent-labeled ligands for imaging PCa

PSMA-targeted small molecule NIR fluorescent dye was first described[116] by conjugation of monomeric GPI ligand to a highly water soluble NIR dye, IRDye78. The conjugate, designated as GPI-78, showed high affinity (9 nM) in vitro in LNCaP cells. Also, for any NIR fluorescent dye to qualify as an intraoperative imaging agent, it should have rapid biodistribution within the tumor and fast clearance rate from nontargeted tissues. Unfortunately, in vivo examination of mouse model bearing LNCaP tumor xenograft showed that GPI-78 NIR conjugate had a total tumor uptake of only 0.06% ID/g 4 hours postinjection. The minimal uptake in the tumor combined with fast renal clearance rate led to the poor performance of GPI-78 molecule during in vivo imaging studies. The reasons for failure were attributed to the small size of GPI-78 and competitive inhibition by other endogenous phosphate ligands present in the blood serum. A possible solution to circumvent these drawbacks would be to increase the size of fluorescent probe along with attachment of multiple GPI ligands to a central template as described earlier.[82] Indeed, several trimerized GPI conjugates of IR800CW dye were later synthesized[117] and found to exhibit sub nanomolar binding affinity to PCa cells thereby rendering them as a possible candidate for in vivo imaging. A phosphoramidate peptidomimetic inhibitor of PSMA conjugated to fluorescein dye has been described to show PSMA-binding specificity and intracellular localization in vitro in LNCaP cells.[118]

Urea-based fluorescent-labeled ligands for optical imaging of PCa

Following the use of phosphate ligand (GPI) conjugation with NIR dyes, next in line to be explored for anti-PSMA activity were urea-based PSMA ligands. Recently, using Lys-NHCONH-Glu as a targeting ligand for PSMA protein, a new anti-PSMA NIR conjugate (YC-27) was synthesized with IR800CW dye and evaluated for in vitro and in vivo imaging studies.[119] YC-27 conjugate was demonstrated to exhibit high binding affinity (K_d = 0.37 nM) during in vivo imaging on SCID mouse bearing PSMA$^+$ PC3-PIP tumor (Figure 15). This preliminary investigation resulted in the development of real-time NIR laparoscopic imaging, using YC-27 NIR conjugate, to detect and surgically remove PSMA positive xenografts in murine and porcine models to reduce positive surgical margins (PSM).[120] The study has stimulated a surge of interest to develop new small molecule NIR imaging agents for intraoperative guided PCa surgery.

PSMA-targeted urea-based DUPA-rhodamine and DUPA-fluorescein conjugates were also developed and shown to exhibit high binding affinity in LNCaP cells using flow cytometry studies.[85] Even though presence of tumor cells were discovered in the blood stream of advanced cancer patients a century ago, but only recently new methods become available to detect these cells in the patients with cancer. The presence of circulating tumor cells (CTCs) in the peripheral

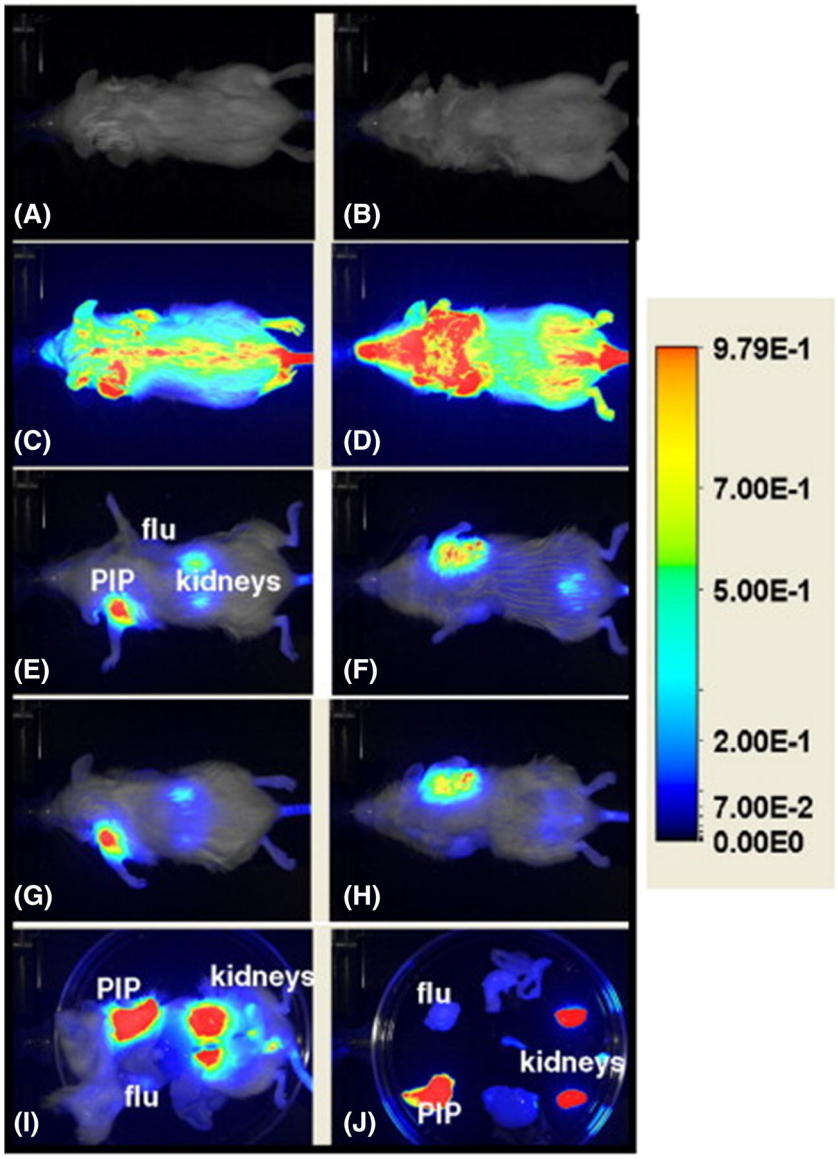

FIGURE 15 Shows the in vivo imaging of an immunocompromised mouse bearing PC3-PIP (forward left flank) and PC3-flu (forward right flank) tumors using NIR conjugate (YC-27) synthesized with IR800CW dye. Dosage injected was 1 nmol and dorsal and ventral views of the preinjection image (A,B, respectively) are shown; 10 min PI (C,D); 20.5 h (E,F); and 24 h (G,H). Images (I) and (J) show after midline laparotomy and individually harvested organs on a Petri dish at 24 h PI, respectively. Reproduced with permission from Chen et al[119]

blood of patients with metastatic cancer has been found to be of prognostic significance, and changes in CTC numbers over time reflect the outcome of any cancer therapy. Interestingly, DUPA-fluorescein conjugate has been shown to bind and label such circulating tumor cells in fresh peripheral blood samples from the PCa patients. Therefore, DUPA-fluorescent conjugates could be used to assess tumor burden or recurrent disease in PCa patients.[121] Complete surgical resection of malignant disease by fluorescence-guided surgery upon intravenous injection of DUPA ligand conjugated anti-PSMA NIR fluorescent agents[122] such as DUPA-Alexafluor 647 or DyLight 680 on tumor-bearing mouse with metastatic PCa has successfully laid the foundation for future fluorescence-guided surgery in a clinical scenario in humans (Figure 16).

3.3 | Miscellaneous PSMA imaging methods

3.3.1 | Functionalized nanoparticles for imaging of PCa

PSMA-specific small molecule ligands can also be attached to nanoparticles for selective and enhanced delivery of a high payload of therapeutic drugs to PCa cells. Nanoparticles are known to passively accumulate within the tumor interstitium due to enhanced permeability and retention effect (EPR). When the nanoparticles are decorated with PSMA-specific ligands, the accumulation effect becomes both specific and longer leading to considerable therapeutic effect. This principle has been demonstrated recently for both diagnosis and

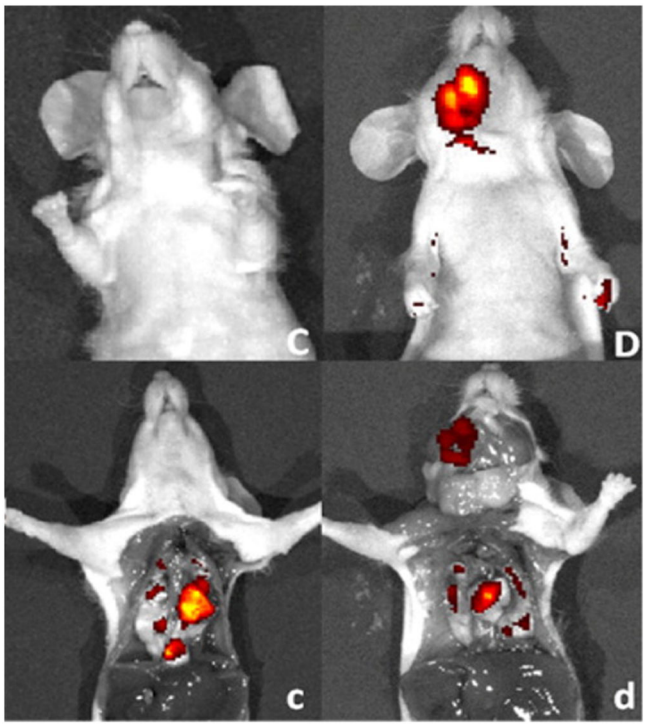

FIGURE 16 Fluorescent images of mice with metastatic disease 4 h following intravenous injection of DUPA-NIR probes. Fluorescent and white light image overlays of intact (C,D) and surgically opened (c,d) tumor-bearing mice. Mice (athymic nu/nu strain) with PSMA-expressing 22RV1 tumors were injected intravenously with 10 nmol of either DUPA-Dylight 680 (C/c) or DUPA-Alexafluor 647 (D/d) and imaged 4 h postinjection. Reprinted (adapted) with permission from Kelderhouse et al[122]

therapy of PCa cells using fluorescently labeled ligands and drug-loaded nanoparticles.[123]

3.3.2 | Peptides and oligonucelotides or aptamers for targeting PCa

Small peptides that bind selectively to PSMA cells can also be used to deliver cytotoxic drugs, protein toxins, and viruses selectively to target sites while minimizing systemic toxicity to healthy tissues. Compared with antibody-based imaging agents, small size peptides are cost-effective, nonimmunogenic and can be coupled with ease to imaging or cytotoxic agents. For example, from a library of linear 12 amino acid peptides, a peptide sequence, WQPDTAHHWATL, was identified to selectively bind $PSMA^+$ cells.

Unlike other PSMA-binding moieties, a dimeric version of this peptide has been shown to inhibit PSMA enzyme activity in micromolar concentration (IC_{50} = 2.2 μM).[124-126] Moreover, peptides and their derivatives are highly susceptible to proteolytic cleavage by endogenous enzymes like peptidases present in the serum. Therefore, other alternatives with better serum stability such as oligonucleotides are preferred that could selectively bind to a given target. These oligonucleotides, called "aptamers," are emerging as a new class of targeting ligands when compared with established antibodies and small molecule ligands.

Belonging to such a family of ligands, recently two oligonucleotides (xPSM-A9 and xPSM-A10)[127] that bind selectively to the extracellular domain of PSMA have been identified and characterized for detection of PCa. Aptamer, xPSM-A9 binds noncompetitively (K_i = 2.1 nM) whereas xPSM-A10 in a competitive mode (K_i = 11.9 nM) to PSMA protein. The different modes of binding of aptamer suggest that each aptamer recognizes a unique extracellular epitope of PSMA. It was also found that one of the truncated aptamers specifically binds to LNCaP cells expressing PSMA but not to PSMA-devoid PC-3 cancer cells. These are the first RNA aptamers reported to bind a prostate tumor-associated membrane antigen, PSMA and can be modified to deliver imaging and therapeutic agents directed against PCa cells.

Motivated by the desirable specific binding affinity of RNA aptamers to PSMA, several investigations were conducted later by employing aptamers conjugated to fluorescent nanocrystals and metallic nanoparticles as imaging agents. In one of the studies, nuclease stable biotinylated RNA aptamer A9 was conjugated to streptavidin coated CdSe or CdTe nanocrystals and tested for in vitro uptake in LNCaP cells using fluorescent microscopy.[128] Fluorescent images obtained from live and fixed cells, and cells grown on a collagen matrix, mimicking real tissues, showed PSMA receptor mediated uptake of the aptamer conjugates. These initial studies were found to be very promising and revealed the hidden potential applications of the aptamer-nanocrystal conjugates for in vivo imaging studies. However, prior knowledge of metal cytotoxicity and biodistribution of conjugates may predispose failure of in vivo applications of aptamer-nanocrystal conjugates. To minimize the toxicity associated with heavy metal nanocrystal imaging agents, oligonucleotide coated gold nanoparticle-aptamer conjugates were an alternative. This was demonstrated during one of the uptake studies of A9 RNA aptamer-oligonucleotide gold nanoparticle conjugate in LNCap cell line using reflectance imaging studies. The conjugation of the aptamer to the oligonucleotide coated gold nanoparticles was achieved via a complementary sequence extension present in the aptamer.[129]

Hybridization of semiconductor nanocrystals called quantum dots (QDs) with aptamer (A10 RNA) and chemotherapeutic drug to produce QD-Aptamer-Drug conjugate (QD-Apt-Drug) has been demonstrated for simultaneous in vitro PCa detection and therapeutic applications. The aptamer performs dual role of carrying the chemotherapeutic drug and targeting the PSMA enzyme while QD acts as fluorescent imaging vehicle carrier.[130] Confocal microscopy study has shown considerable uptake of QD-Apt-Drug conjugate in LNCaP cells by PSMA mediated endocytosis. Based on the same principle, a magnetic resonance contrast agent, superparamagnetic iron oxide nanoparticle (SPION) in conjugation with aptamer-drug (SPION-Apt-Drug) has been demonstrated in vitro to identify and treat PCa cells.[131] Ferumoxtran-10 (Combidex), a dextran-coated SPION is currently under phase III clinical trials for PCa imaging.[132]

Comparison of peptides and oligonucleotides or aptamers (Table 1) will help the reader to decide on the selection of targeting moieties derived from peptides or aptamers as per the requirements.

TABLE 1 Advantages and disadvantages of targeting peptides and oligonucleotides or aptamers for PCa imaging

S. No.	Property	Peptides	Oligonucleotides or Aptamers
1.	Ease of synthesis and manufacturing	Peptide analogs are synthesized by established solid-phase peptide synthesis (SPPS) methods, which produces reproducible constructs with accurate chemical structures. Production cost for bulk manufacturing is considerably lower than for monoclonal antibody and aptamers.[133]	Easy, reliable, and automated methods for synthesis of aptamers are available, which also easily facilitate chemical modifications like attachment points to tether enzymes. However, manufacturing costs are high as the technology has not yet evolved to generate large amounts within reasonable costs.[134]
2.	Metabolic or serum stability	Targeting peptides are generally metabolically unstable as they can be easily digested by proteases present in the blood plasma and are prone to fast renal clearance. They are also susceptible to endopeptidases and exopeptidases present in the tissues. This sometimes results in loss of bioactivity even before reaching the intended target.	Aptamers also have low metabolic stability and circulation half-life (~2 min) due to susceptibility to nuclease degradation.
3.	Target specificity	Peptides have high affinity and specificity to a target protein as they are identified after extensive screening with a library by phage display technology.[135]	Aptamers also show high target specificity as they are identified by an in vitro selection process, systematic evolution of ligands by exponential enrichment (SELEX), which can be monitored to tailor affinities according to a protein target.
4.	Penetration and uptake in tumor tissues	Its small size in comparison with proteins (<50 amino acids) enables good tissue penetration and uptake in tumors.	Shows good tumor penetration due to its small size (3000-20 000 Da), but comparably less efficient than small molecule targeting ligands.[136]

3.3.3 | QDs conjugated PCa optical imaging probes

QDs are also conjugated to intact mAb or engineered antibody fragments for detection of PCa. The former case is illustrated by conjugating NIR QD probe, Qdot-800, to an extensively studied PSMA mAb J591. NIR QD probes would show deep tissue tumors more clearly due to minimal tissue autofluorescence in the NIR region. Therefore, in vivo fluorescent images of mouse bearing C4-2 and C4-2B human prostate tumors in bone using Qdot-800-J591 conjugate are found to be far superior when compared with other optical imaging agents.[137] However, monoclonal antibodies are large (100-150 kDa) and eliminate slowly from serum creating considerable background interferences. In such instances, engineered antibodies called diabodies that retain binding specificity with the target antigen and exhibit fast clearance from nontargeted tissues are preferred for in vivo applications. This principle was recently exemplified[138] using a pegylated QD conjugate, cys-Diabody-CdSe/ZnS, for in vitro applications in LNCaP or prostate stem cell antigen (PSCA) cells.

4 | CONCLUSION

Prostate-specific membrane antigen (PSMA) is a transmembrane glycoprotein showing overexpression in PCa tissues. Currently, enormous efforts are being made to develop homing moieties that exclusively target PSMA with high specificity and affinity. This report extensively describes and compares the various targeting moieties derived from monoclonal antibodies, small molecule ligands, peptides, peptide derivatives, and aptamers for bio-imaging of PCa cells. mAb imaging agents such as "ProstaScint" was approved by the FDA for metastatic noninvasive imaging of prostate tumor despite several known disadvantages. Among all the targeting motifs, small molecule ligands show enormous potential as homing moieties to deliver imaging agents. Two major classes of small molecule ligands have been discovered to be successful as targeted diagnostic agents for detection of PCa. The first kind, phosphorous ligands, conjugated with NIR fluorescent dyes were explored as potential intraoperative agents to detect and treat PCa but failed during in vivo mouse model studies due to poor tumor uptake and fast renal clearance rate. Phosphorous ligands are difficult to purify and are also unstable in acidic and basic medium. They are also prone to attack by nucleophiles in the system leading to side reactions and loss of affinity. Another well-studied classes of successful small molecule ligands are urea-based inhibitors, which when conjugated to radioisotopes or fluorescent dyes show high affinity for detection of PCa. Urea-based ligands are simple to prepare, stable in acidic, and basic medium. They can be easily conjugated to chelating linkers like DOTA, NOTA, peptide sequestering moiety (EC-20) during solid-phase peptide synthesis to deliver radionuclides for diagnosis and therapy compared with phosphorous ligands. The radionuclear conjugates derived from urea-based ligands have shown excellent results both in preclinical and clinical trails to detect PCa. Additionally, the NIR fluorescent conjugates derived from urea-based ligands were proved to be successful intraoperative guided tool during cancer surgery for optimum resection of residual tumors in cancer patients. Peptides and aptamers have also been studied as PCa targeting moieties, but they fail to elicit expected clinical success due to low circulation time and instability in blood plasma. Finally, this report provides an in-depth analysis of different PSMA targeting moieties, their stabilities, production costs, ease of preparation, tumor uptake, rate of renal clearance, scan time, sensitivity, merits, and demerits in preclinical and clinical scenarios, for successful diagnosis of PCa.

ACKNOWLEDGMENTS

The authors are thankful to Ministry of Human Resource Development (MHRD), Government of India and Indian Institute of Technology (IIT) Indore, India, for research funding and student's research fellowships.

AUTHORS' CONTRIBUTIONS

All authors had full access to the data in the study and take responsibility for the integrity of the data and the accuracy of the data analysis. *Conceptualization*, V.C.; *Methodology*, V.C.; *Investigation*, V.C.; *Formal Analysis*, V.C., S.S., M.A.K., S.C.; *Resources*, V.C., S.C.; *Writing - Original Draft*, V.C.; *Writing - Review & Editing*, V.C., M.A.K., S.S., S.C.; *Visualization*, V.C.; *Supervision*, V.C.; *Funding Acquisition*, V.C.

CONFLICT OF INTERESTS

The authors have stated explicitly that there are no conflicts of interest in connection with this article.

ETHICS APPROVAL AND CONSENT TO PARTICIPATE

Experimental research on small animals complies with institutional, national, or international guidelines, and articles cited in this report were selected on the basis of the original declaration and practice of animal ethics protocol as per international guidelines. Permissions were sought from authors or publishers to publish figures involving animal experiments or clinical trials and please see Supporting Information for details.

ORCID

Venkatesh Chelvam https://orcid.org/0000-0001-9593-3759

REFERENCES

1. Hricak H, Choyke PL, Eberhardt SC, Leibel SA, Scardino PT. Imaging prostate cancer: a multidisciplinary perspective. *Radiology*. 2007;243(1):28-53.
2. Wester H-J. Nuclear imaging probes: from bench to bedside. *Clin. Cancer Res.* 2007;13(12):3470-3481.
3. Mueller-Lisse UG, Scherr MK. Proton MR spectroscopy of the prostate. *Eur. J. Radiol.* 2007;63(3):351-360.
4. Cancer projected to become leading cause of death worldwide in 2010. 2008;1–5.
5. Siegel R, Miller KD, Ahmedin J. Cancer statistics. *CA Cancer J. Clin.* 2017;67(1):7-30.
6. Wilson LS, Tesoro R, Elkin EP, et al. Cumulative cost pattern comparison of prostate cancer treatments. *Cancer*. 2007;109(3):518-527.
7. Katz A. Quality of life for men with prostate cancer. *Cancer Nurs.* 2007;30(4):302-308.
8. Chistiakov DA, Myasoedova VA, Grechko AV, Melnichenko AA, Orekhov AN. New biomarkers for diagnosis and prognosis of localized prostate cancer. *Semin. Cancer Biol.* 2018;52(1):9-16.
9. Kiess AP, Banerjee SR, Mease RC, et al. Prostate-specific membrane antigen as a target for cancer imaging and therapy. *J Nucl Med Mol Imaging*. 2015;59(3):241-268.
10. Wüstemann T, Haberkorn U, Babich J, Mier W. Targeting prostate cancer: prostate-specific membrane antigen based diagnosis and therapy. *Med. Res. Rev.* 2018;39:1-30.
11. Afaq A, Batura D, Bomanji J. New frontiers in prostate cancer imaging: clinical utility of prostate-specific membrane antigen positron emission tomography. *Int. Urol. Nephrol.* 2017;49(5):803-810.
12. Bjurlin MA, Turkbey B, Rosenkrantz AB, Gaur S, Choyke PL, Taneja SS. Imaging the high-risk prostate cancer patient: current and future approaches to staging. *Urology*. 2018;116:3-12.
13. Sanchez-Crespo A. Comparison of gallium-68 and fluorine-18 imaging characteristics in positron emission tomography. *Appl. Radiat. Isot.* 2013;76:55-62.
14. Wallitt KL, Khan SR, Dubash S, Tam HH, Khan S, Barwick TD. Clinical PET imaging in prostate cancer. *Radiographics*. 2017;37(5):1512-1536.
15. Jadvar H. Molecular imaging of prostate cancer: PET radiotracers. *Am. J. Roentgenol.* 2012;199(2):278-291.
16. Lenzo N, Meyrick D, Turner J. Review of gallium-68 PSMA PET/CT imaging in the management of prostate cancer. *Diagnostics*. 2018;8(1):1-17.
17. Pillai MRA, Nanabala R, Joy A, Sasikumar A, Russ Knapp FF. Radiolabeled enzyme inhibitors and binding agents targeting PSMA: effective theranostic tools for imaging and therapy of prostate cancer. *Nucl. Med. Biol.* 2016;43(11):692-720.
18. Kratochwil C, Afshar-Oromieh A, Kopka K, Haberkorn U, Giesel FL. Current status of prostate-specific membrane antigen targeting in nuclear medicine: clinical translation of chelator containing prostate-specific membrane antigen ligands into diagnostics and therapy for prostate cancer. *Semin. Nucl. Med.* 2016;46(5):405-418.
19. Haberkorn U, Eder M, Kopka K, Babich JW, Eisenhut M. New strategies in prostate cancer: prostate-specific membrane antigen (PSMA) ligands for diagnosis and therapy. *Clin. Cancer Res.* 2016;22(1):9-15.
20. Zeller JL. Grading of prostate cancer. *JAMA*. 2015;298:1596.
21. Essink-Bot ML, de Koning HJ, Nijs HG, Kirkels WJ, van der Maas PJ, Schröder FH. Short-term effects of population-based screening for prostate cancer on health-related quality of life. *J. Natl. Cancer Inst.* 1998;90(12):925-931.
22. Chodak GW, Keller P, Schoenberg HW. Assessment of screening for prostate cancer using the digital rectal examination. *J. Urol.* 1989;141(5):1136-1138.
23. Linn MM, Ball RA, Maradiegue A. Prostate-specific antigen screening: friend or foe? *Urol. Nurs.* 2007;27(6):481-489.
24. D'Amico AV, Roehrborn CG. Effect of 1 mg/day finasteride on concentrations of serum prostate-specific antigen in men with androgenic alopecia: a randomised controlled trial. *Lancet Oncol.* 2007;8(1):21-25.
25. Wefer AE, Hricak H, Vigneron DB, et al. Sextant localization of prostate cancer: comparison of sextant biopsy, magnetic resonance imaging and magnetic resonance spectroscopic imaging with step section histology. *J. Urol.* 2000;164(2):400-404.
26. Zakian KL, Sircar K, Hricak H, et al. Correlation of proton MR spectroscopic imaging with Gleason score based on step-section pathologic analysis after radical prostatectomy. *Radiology*. 2005;234(3):804-814.
27. Wolf JSJ, Cher M, Dall'era M, Presti JCJ, Hricak H, Carroll PR. The use and accuracy of cross-sectional imaging and fine needle aspiration cytology for detection of pelvic lymph node metastases before radical prostatectomy. *J. Urol.* 1995;153(3):993-999.
28. Hövels AM, Heesakkers RAM, Adang EM, et al. The diagnostic accuracy of CT and MRI in the staging of pelvic lymph nodes in patients with prostate cancer: a meta-analysis. *Clin. Radiol.* 2008;63(4):387-395.
29. Horoszewicz JS, Kawinski E, Murphy GP. Monoclonal antibodies to a new antigenic marker in epithelial prostatic cells and serum of prostatic cancer patients. *Anticancer Res.* 1987;7(5B):927-935.

30. Israeli RS, Powell CT, Corr JG, Fair WR, Heston WDW. Expression of the prostate-specific membrane antigen expression of the prostate-specific embrane antigen. *Cancer Res.* 1994;54:1807-1811.
31. Tricoli JV, Schoenfeldt M, Conley BA, Tricoli JV, Schoenfeldt M, Conley BA. Detection of prostate cancer and predicting progression: current and future diagnostic markers. *Clin. Cancer Res.* 2004;10(301):3943-3953.
32. Rajasekaran AK, Anilkumar G, Christiansen JJ. Is prostate-specific membrane antigen a multifunctional protein? *Am. J. Physiol. Cell Physiol.* 2005;288(67):975-981.
33. Gong MC, Chang SS, Sadelain M, Bander NH, Heston WD. Prostate-specific membrane antigen (PSMA)-specific monoclonal antibodies in the treatment of prostate and other cancers. *Cancer Metastasis Rev.* 1999;18(4):483-490.
34. Mesters JR, Barinka C, Li W, et al. Structure of glutamate carboxypeptidase II, a drug target in neuronal damage and prostate cancer. *EMBO J.* 2006;25(6):1375-1384.
35. Davis MI, Bennett MJ, Thomas LM, Bjorkman PJ. Crystal structure of prostate-specific membrane antigen, a tumor marker and peptidase. *Proc. Natl. Acad. Sci. U. S. A.* 2005;102(17):5981-5986.
36. Ghosh A, Heston WDW. Tumor target prostate specific membrane antigen (PSMA) and its regulation in prostate cancer. *J. Cell. Biochem.* 2004;91(3):528-539.
37. Silver DA, Pellicer I, Fair WR, Heston WD, Cordon-Cardo C. Prostate-specific membrane antigen expression in normal and malignant human tissues. *Clin. Cancer Res.* 1997;3(1):81-85.
38. Chang SS, Reuter VE, Heston WDW, Bander NH, Grauer LS, Gaudin PB. Five different anti-prostate-specific membrane antigen (PSMA) antibodies confirm PSMA expression in tumor-associated neovasculature. *Cancer Res.* 1999;59(13):3192-3198.
39. Kawakami M, Nakayama J. Enhanced expression of the prostate specific membrane antigen gene in prostate cancer as revealed by in situ hybridization. *Cancer Res.* 1997;57(12):231-234.
40. Ross JS, Sheehan CE, Fisher HAG, et al. Correlation of primary tumor prostate-specific membrane antigen expression with disease recurrence in prostate cancer. *Clin. Cancer Res.* 2003;9(17):6357-6362.
41. Wright GL, Grob BM, Haley C, et al. Upregulation of prostate-specific membrane antigen after androgen-deprivation therapy. *Urology*. 1996;48(2):326-334.
42. Sweat SD, Pacelli A, Murphy GP, Bostwick DG. Prostate-specific membrane antigen expression is greatest in prostate adenocarcinoma and lymph node metastases. *Urology*. 1998;52(4):637-640.
43. Chang SS, Reuter VE, Heston WDW, Gaudin PB. Comparison of anti-prostate-specific membrane antigen antibodies and other immunomarkers in metastatic prostate carcinoma. *Urology*. 2001;57(6):1179-1183.
44. Murphy GP, Barren RJ, Erickson SJ, et al. Evaluation and comparison of two new prostate carcinoma markers: free-prostate specific antigen and prostate specific membrane antigen. *Cancer*. 1996;78(1):809-818.
45. Lopes AD, Davis WL, Rosenstraus MJ, Uveges AJ, Gilman SC. Immunohistochemical and pharmacokinetic characterization of the site-specific immunoconjugate CYT-356 derived from antiprostate monoclonal antibody 7E11-C5. *Cancer Res.* 1990;50(19):6423-6429.
46. Troyer JK, Beckett ML, Wright GL. Detection and characterization of the prostate-specific membrane antigen (PSMA) in tissue extracts and body fluids. *Int. J. Cancer*. 1995;62(5):552-558.
47. Chang SS, Keefe DSO, Bacich DJ, Reuter VE, Heston WDW, Gaudin PB. Prostate-specific membrane antigen is produced in tumor-associated neovasculature. *Clin. Cancer Res.* 1999;5(10):2674-2681.
48. Tasch J, Gong M, Sadelain M, Heston WD. A unique folate hydrolase, prostate-specific membrane antigen (PSMA): a target for immunotherapy? *Crit. Rev. Immunol.* 2001;21(1–3):249-261.
49. Liu S, Edwards DS. ^{99m}Tc-labeled small peptides as diagnostic radiopharmaceuticals. *Chem. Rev.* 1999;99(9):2235-2268.
50. Rosenstraus MJ. In vitro and in vivo reactivity of anti-prostate monoclonal antibody immunoconjugate 7E11.C5.3 GYK-DTPA. *Radiopharmaceuticals*. 1990;3:54-60.
51. Wynant GE, Murphy GP, Horoszewicz JS, et al. Immunoscintigraphy of prostatic cancer: preliminary results with ^{111}In-labeled monoclonal antibody 7E11-C5.3 (CYT-356). *Prostate*. 1991;18(3):229-241.
52. Murphy GP, Elgamal A-AA SSL, Bostwick DG, Holmes EH. Current evaluation of the tissue localization and diagnostic utility of prostate specific membrane antigen. *Cancer*. 1998;83(11):2259-2269.
53. Abdel-Nabi H, Wright GL, Gulfo JV, et al. Monoclonal antibodies and radioimmunoconjugates in the diagnosis and treatment of prostate cancer. *Semin. Urol.* 1992;10(1):45-54.
54. Babaian RJ, Sayer J, Podoloff DA, Steelhammer LC, Bhadkamkar VA, Gulfo JV. Radioimmunoscintigraphy of pelvic lymph nodes with^{111}Indium-labeled monoclonal antibody CYT-356. *J. Urol.* 1994;152(6):1952-1955.
55. Kahn D, Williams RD, Seldin DW, et al. Radioimmunoscintigraphy with ^{111}Indium labeled CYT-356 for the detection of occult prostate cancer recurrence. *J. Urol.* 1994;152(5):1490-1495.
56. Burgers JK, Hinkle GH, Haseman MK. Monoclonal antibody imaging of recurrent and metastatic prostate cancer. *Semin. Urol.* 1995;13(2):103-112.
57. Feneley MR, Jan H, Granowska M, et al. Imaging with prostate-specific membrane antigen (PSMA) in prostate cancer. *Prostate Cancer Prostatic Dis.* 2000;3(1):47-52.
58. Han M, Partin AW. Current clinical applications of the ^{111}In-capromab pendetide scan (ProstaScint® Scan, Cyt-356). *Rev. Urol.* 2001;3(4):165-171.
59. Ponsky LE, Cherullo EE, Starkey R, Nelson D, Neumann D, Zippe CD. Evaluation of preoperative ProstaScint scans in the prediction of nodal disease. *Prostate Cancer Prostatic Dis.* 2002;5(2):132-135.
60. Sodee DB, Ellis RJ, Samuels MA, et al. Prostate cancer and prostate bed SPECT imaging with ProstaScint: semiquantitative correlation with prostatic biopsy results. *Prostate*. 1998;37(3):140-148.
61. Boyer BP, Boyer MJ. An elusive tumor in a man who has evidence of prostate cancer metastasis. *JAAPA*. 2009;22(8):22-25.
62. Lee Z, Sodee DB, Resnick M, MacLennan GT. Multimodal and three-dimensional imaging of prostate cancer. *Comput. Med. Imaging Graph.* 2005;29(6):477-486.
63. Feneley MR, Chengazi VU, Kirby RS, et al. Prostatic radioimmunoscintigraphy: preliminary results using technetium-labelled monoclonal antibody, CYT-351. *Br. J. Urol.* 1996;77(3):373-381.
64. Chengazi VU, Feneley MR, Ellison D, et al. Imaging prostate cancer with technetium-99m-7E11-C5.3 (CYT-351). *J. Nucl. Med.* 1997;38(5):675-682.
65. Stalteri MA, Mather SJ, Belinka BA, Coughlin DJ, Chengazi VU, Britton KE. Site-specific conjugation and labelling of prostate antibody 7E11C5.3 (CYT-351) with technetium-99m. *Eur. J. Nucl. Med.* 1997;24(6):651-654.
66. Liu H, Moy P, Kim S, et al. Monoclonal antibodies to the extracellular domain of prostate-specific membrane antigen also react with tumor vascular endothelium. *Cancer Res.* 1997;57(17):3629-3634.
67. Hamilton A, King S, Liu H, Moy P, Bander N, Carr F. A novel humanised antibody against prostate specific membrane antigen (PSMA) for in vivo targeting and therapy. *Proc Am Assoc Cancer Res Annu Meet*. 1998;39:440.
68. Liu H, Rajasekaran AK, Moy P, et al. Constitutive and antibody-induced internalization of prostate-specific membrane antigen. *Cancer Res.* 1998;58(18):4055-4060.

69. Milowsky MI, Nanus DM, Kostakoglu L, Vallabhajosula S, Goldsmith SJ, Bander NH. Phase I trial of yttrium-90-labeled anti-prostate-specific membrane antigen monoclonal antibody J591 for androgen-independent prostate cancer. *J. Clin. Oncol.* 2004;22(13):2522-2531.
70. Bander NH, Milowsky MI, Nanus DM, Kostakoglu L, Vallabhajosula S, Goldsmith SJ. Phase I trial of ^{177} lutetium-labeled J591, a monoclonal antibody to prostate-specific membrane antigen, in patients with androgen-independent prostate cancer. *J. Clin. Oncol.* 2005;23(21):4591-4601.
71. Milowsky MI, Nanus DM, Kostakoglu L, et al. Vascular targeted therapy with anti-prostate-specific membrane antigen monoclonal antibody J591 in advanced solid tumors. *J. Clin. Oncol.* 2007;25(5):540-547.
72. Morris MJ, Pandit-Taskar N, Divgi CR, et al. Phase I evaluation of J591 as a vascular targeting agent in progressive solid tumors. *Clin. Cancer Res.* 2007;13(9):2707-2713.
73. Elsasser-Beile U, Wolf P, Gierschner D, Buhler P, Schultze-Seemann W, Wetterauer U. A new generation of monoclonal and recombinant antibodies against cell-adherent prostate specific membrane antigen for diagnostic and therapeutic targeting of prostate cancer. *Prostate*. 2006;66(13):1359-1370.
74. Elsasser-Beile U, Reischl G, Wiehr S, et al. PET imaging of prostate cancer xenografts with a highly specific antibody against the prostate-specific membrane antigen. *J. Nucl. Med.* 2009;50(4):606-611.
75. Jin H, Xu M, Padakanti PK, Liu Y, Lapi S, Tu Z. Preclinical evaluation of the novel monoclonal antibody H6-11 for prostate cancer imaging. *Mol. Pharm.* 2013;10(10):3655-3664.
76. Gambhir SS, Yaghoubi SS. *Molecular Imaging with Reporter Genes*. Cambridge University Press; 2010:120. http://doi.org/10.1017/CB09780511730405.004
77. Friedrich SW, Linz SC, Stoll BR, Baxter LT, Munn LL, Jain RK. Antibody-directed effector cell therapy of tumors: analysis and optimization using a physiologically based pharmacokinetic model. *Neoplasia*. 2002;4(5):449-463.
78. Seccamani E, Tattanelli M, Mariani M, Spranzi E, Scassellati GA, Siccardi AG. A simple qualitative determination of human antibodies to murine immunoglobulins (HAMA) in serum samples. *Int. J. Rad. Appl. Instrum. A*. 1989;16(2):167-170.
79. Colcher D, Bird R, Roselli M, et al. In vivo tumor targeting of a recombinant single-chain antigen-binding protein. *J. Natl. Cancer Inst*. 1990;82(14):1191-1197.
80. Viola-Villegas NT, Sevak KK, Carlin SD, et al. Noninvasive imaging of PSMA in prostate tumors with ^{89}Zr-labeled huJ591 engineered antibody fragments: the faster alternatives. *Mol. Pharm.* 2014;11(11):3965-3973.
81. Velikyan I. Prospective of ^{68}Ga-radiopharmaceutical development. *Theranostics*. 2014;4(1):47-80.
82. Misra P, Humblet V, Pannier N, Maison W, John V. Production of multimeric prostate-specific membrane antigen small molecule radiotracers using a solid-phase ^{99m}Tc pre-loading strategy. *J. Nucl. Med.* 2007;48(8):1379-1389.
83. Banerjee SR, Foss CA, Castanares M, et al. Synthesis and evaluation of technetium-99m- and rhenium-labeled inhibitors of the prostate-specific membrane antigen (PSMA). *J. Med. Chem.* 2008;51(15):4504-4517.
84. Kularatne SA, Zhou Z, Yang J, Post CB, Low PS. Design, synthesis, and preclinical evaluation of prostate-specific membrane antigen targeted ^{99m}Tc-radioimaging agents. *Mol. Pharm.* 2009;6(3):790-800.
85. Kularatne SA, Wang K, Santhapuram H-KR, Low PS. Prostate-specific membrane antigen targeted imaging and therapy of prostate cancer using a PSMA inhibitor as a homing ligand. *Mol. Pharm.* 2009;6(3):780-789.
86. Banerjee SR, Pullambhatla M, Byun Y, et al. ^{68}Ga-labeled inhibitors of prostate-specific membrane antigen (PSMA) for imaging prostate cancer. *J. Med. Chem.* 2010;53(14):5333-5341.
87. Eder M, Schäfer M, Bauder-Wüst U, et al. ^{68}Ga-complex lipophilicity and the targeting property of a urea-based PSMA inhibitor for PET imaging. *Bioconjug. Chem.* 2012;23(4):688-697.
88. Afshar-Oromieh A, Haberkorn U, Eder M, Eisenhut M, Zechmann CM. [^{68}Ga]gallium-labelled PSMA ligand as superior PET tracer for the diagnosis of prostate cancer: comparison with ^{18}F-FECH. *Eur. J. Nucl. Med. Mol. Imaging*. 2012;39(6):1085-1086.
89. Afshar-Oromieh A, Zechmann CM, Malcher A, et al. Comparison of PET imaging with a ^{68}Ga-labelled PSMA ligand and ^{18}F-choline-based PET/CT for the diagnosis of recurrent prostate cancer. *Eur. J. Nucl. Med. Mol. Imaging*. 2014;41(1):11-20.
90. Afshar-Oromieh A, Malcher A, Eder M, et al. PET imaging with a [^{68}Ga]gallium-labelled PSMA ligand for the diagnosis of prostate cancer: biodistribution in humans and first evaluation of tumour lesions. *Eur. J. Nucl. Med. Mol. Imaging*. 2013;40(4):486-495.
91. Weineisen M, Schottelius M, Simecek J, et al. ^{68}Ga- and ^{177}Lu-labeled PSMA-I&T: optimization of a PSMA-targeted theranostic concept and first proof-of-concept human studies. *J. Nucl. Med.* 2015;56(8):1169-1176.
92. Schottelius M, Wirtz M, Eiber M, Maurer T, Wester HJ. [^{111}In]PSMA-I&T: expanding the spectrum of PSMA-I&T applications towards SPECT and radioguided surgery. *Eur. J. Nucl. Med. Mol. Imaging*. 2015;5(1):1-5.
93. Delker A, Fendler WP, Kratochwil C, et al. Dosimetry for 177Lu-DKFZ-PSMA-617: a new radiopharmaceutical for the treatment of metastatic prostate cancer. *Eur. J. Nucl. Med. Mol. Imaging*. 2016;43(1):42-51.
94. Chen Y, Foss CA, Byun Y, et al. Radiohalogenated prostate-specific membrane antigen (PSMA)-based ureas as imaging agents for prostate cancer. *J. Med. Chem.* 2008;51(24):7933-7943.
95. Maresca KP, Hillier SM, Femia FJ, et al. A series of halogenated heterodimeric inhibitors of prostate specific membrane antigen (PSMA) as radiolabeled probes for targeting prostate cancer. *J. Med. Chem.* 2009;52(2):347-357.
96. Hillier SM, Maresca KP, Femia FJ, et al. Preclinical evaluation of novel glutamate-urea-lysine analogs that target prostate specific membrane antigen as molecular imaging pharmaceuticals for prostate cancer. *Cancer Res.* 2009;69(17):6932-6940.
97. Barrett JA, Coleman RE, Goldsmith SJ, et al. First-in-man evaluation of 2 high-affinity PSMA-avid small molecules for imaging prostate cancer. *J. Nucl. Med.* 2013;54(3):380-387.
98. Foss CA, Mease RC, Fan H, et al. Radiolabeled small-molecule ligands for prostate-specific membrane antigen: in vivo imaging in experimental models of prostate cancer. *Clin Cancer*. 2005;11(11):4022-4029.
99. Pomper MG, Musachio JL, Zhang J, et al. ^{11}C-MCG: synthesis, uptake selectivity, and primate PET of a probe for glutamate carboxypeptidase II (NAALADase). *Mol. Imaging*. 2002;1(2):96-101.
100. Mease RC, Dusich CL, Foss CA, et al. N-[N-[(S)-1,3-Dicarboxypropyl] carbamoyl]-4-[^{18}F]fluorobenzyl-L-cysteine, [^{18}F]DCFBC: a new imaging probe for prostate cancer. *Clin. Cancer Res.* 2008;14(10):3036-3043.
101. Cho SY, Gage KL, Mease RC, et al. Biodistribution, tumor detection, and radiation dosimetry of ^{18}F-DCFBC, a low-molecular-weight inhibitor of prostate-specific membrane antigen, in patients with metastatic prostate cancer. *J. Nucl. Med.* 2012;53(12):1883-1891.
102. Chen Y, Pullambhatla M, Foss CA, et al. 2-(3-{1-Carboxy-5-[(6-[18F] fluoro-pyridine-3-carbonyl)-amino]-pentyl}-ureido)-pen tanedioic acid, [^{18}F]DCFPyL, a PSMA-based PET imaging agent for prostate cancer. *Clin. Cancer Res.* 2011;17(24):7645-7653.
103. Szabo Z, Mena E, Rowe SP, et al. Initial evaluation of [^{18}F]DCFPyL for prostate-specific membrane antigen (PSMA)-targeted PET imaging of prostate cancer. *Mol. Imaging Biol.* 2015;17(4):565-574.

104. Rowe SP, Gorin MA, Pomper MG. Imaging of prostate-specific membrane antigen using [^{18}F]DCFPyL. *PET Clin*. 2017;12(3):289-296.
105. Kommidi H, Guo H, Nurili F, et al. ^{18}F-positron emitting/trimethine cyanine-fluorescent contrast for image-guided prostate cancer management. *J. Med. Chem.* 2018;61(9):4256-4262.
106. Harada N, Kimura H, Ono M, Saji H. Preparation of asymmetric urea derivatives that target prostate-specific membrane antigen for SPECT imaging. *J. Med. Chem.* 2013;56(20):7890-7901.
107. Banerjee SR, Pullambhatla M, Foss CA, et al. ^{64}Cu-labeled inhibitors of prostate-specific membrane antigen for PET imaging of prostate cancer. *J. Med. Chem.* 2014;57(6):2657-2669.
108. Lapi SE, Wahnishe H, Pham D, et al. Assessment of an ^{18}F-labeled phosphoramidate peptidomimetic as a new prostate-specific membrane antigen-targeted imaging agent for prostate cancer. *J. Nucl. Med.* 2009;50(12):2042-2048.
109. Maung J, Mallari JP, Girtsman TA, et al. Probing for a hydrophobic a binding register in prostate-specific membrane antigen with phenylalkylphosphonamidates. *Bioorg. Med. Chem.* 2004;12(18):4969-4979.
110. Wu LY, Anderson MO, Toriyabe Y, et al. The molecular pruning of a phosphoramidate peptidomimetic inhibitor of prostate-specific membrane antigen. *Bioorg. Med. Chem.* 2007;15(23):7434-7443.
111. Wu LY, Do JC, Kazak M, et al. Phosphoramidate derivatives of hydroxysteroids as inhibitors of prostate-specific membrane antigen. *Bioorg. Med. Chem. Lett.* 2008;18(1):281-284.
112. Ding P, Helquist P, Miller MJ. Design, synthesis and pharmacological activity of novel enantiomerically pure phosphonic acid-based NAALADase inhibitors. *Org. Biomol. Chem.* 2007;5(5):826-831.
113. Toda M. Intraoperative navigation and fluorescence imagings in malignant glioma surgery. *Keio J. Med.* 2008;57(3):155-161.
114. Frangioni JV. In vivo near-infrared fluorescence imaging. *Curr. Opin. Chem. Biol.* 2003;7(5):626-634.
115. Tanaka E, Choi HS, Fujii H, Bawendi MG, Frangioni JV. Image-guided oncologic surgery using invisible light: completed pre-clinical development for sentinel lymph node mapping. *Ann. Surg. Oncol.* 2006;13(12):1671-1681.
116. Humblet V, Lapidus R, Williams LR, et al. High-affinity near-infrared fluorescent small-molecule contrast agents for in vivo imaging of prostate-specific membrane antigen. *Mol. Imaging*. 2005;4(4):448-462.
117. Humblet V, Misra P, Bhushan KR, et al. Multivalent scaffolds for affinity maturation of small molecule cell surface binders and their application to prostate tumor targeting. *J. Med. Chem.* 2009;52(2):544-550.
118. Liu T, Wu LY, Kazak M, Berkman CE. Cell-surface labeling and internalization by a fluorescent inhibitor of prostate-specific membrane antigen. *Prostate*. 2008;68(9):955-964.
119. Chen Y, Dhara S, Banerjee SR, et al. A low molecular weight PSMA-based fluorescent imaging agent for cancer. *Biochem. Biophys. Res. Commun.* 2009;390(3):624-629.
120. Neuman BP, Eifler JB, Castanares M, et al. Real-time, near-infrared fluorescence imaging with an optimized dye/light source/camera combination for surgical guidance of prostate cancer. *Clin. Cancer Res.* 2015;21(4):771-780.
121. He W, Kularatne SA, Kalli KR, et al. Quantitation of circulating tumor cells in blood samples from ovarian and prostate cancer patients using tumor-specific fluorescent ligands. *Int. J. Cancer*. 2008;123(8):1968-1973.
122. Kelderhouse LE, Chelvam V, Wayua C, et al. Development of tumor-targeted near infrared probes for fluorescence guided surgery. *Bioconjug. Chem.* 2013;24(6):1075-1080.
123. Chandran SS, Banerjee SR, Mease RC, Pomper MG, Denmeade SR. Characterization of a targeted nanoparticle functionalized with a urea-based inhibitor of prostate-specific membrane antigen (PSMA). *Cancer Biol. Ther.* 2008;7(6):974-982.
124. Aggarwal S, Singh P, Topaloglu O, Isaacs JT, Demneade SR. A dimeric peptide that binds selectively to prostate-specific membrane antigen and inhibits its enzymatic activity. *Cancer Res.* 2006;66(18):9171-9177.
125. Lupold SE, Rodriguez R. Disulfide-constrained peptides that bind to the extracellular portion of the prostate-specific membrane antigen. *Mol. Cancer Ther.* 2004;3(5):597-603.
126. Liu C, Huang H, Doñate F, et al. Prostate-specific membrane antigen directed selective thrombotic infarction of tumors. *Cancer Res.* 2002;62(19):5470-5475.
127. Lupold SE, Hicke BJ, Lin Y, Coffey DS. Identification and characterization of nuclease-stabilized RNA molecules that bind human prostate cancer cells via the prostate-specific membrane antigen. *Cancer Res.* 2002;62(14):4029-4033.
128. Chu TC, Shieh F, Lavery LA, et al. Labeling tumor cells with fluorescent nanocrystal-aptamer bioconjugates. *Biosens. Bioelectron.* 2006;21(10):1859-1866.
129. Javier DJ, Nitin N, Levy M, Ellington A, Richards-Kortum R. Aptamer-targeted gold nanoparticles as molecular-specific contrast agents for reflectance imaging. *Bioconjug. Chem.* 2008;19(6):1309-1312.
130. Bagalkot V, Zhang L, Levy-Nissenbaum E, et al. Quantum dot-aptamer conjugates for synchronous cancer imaging, therapy, and sensing of drug delivery based on bi-fluorescence resonance energy transfer. *Nano Lett.* 2007;7(10):3065-3070.
131. Wang AZ, Bagalkot V, Vasilliou CC, et al. Superparamagnetic iron oxide nanoparticle–aptamer bioconjugates for combined prostate cancer imaging and therapy. *Chem Med Chem*. 2008;3(9):1311-1315.
132. Leenders W. Ferumoxtran-10 advanced magnetics. *IDrugs*. 2003;6(10):987-993.
133. Lee S, Xie J, Che X. Peptide-based probes for targeted molecular imaging. *Biochemistry*. 2010;49(7):1364-1376.
134. Ferreira CSM, Missailidis S. Aptamer-based therapeutics and their potential in radiopharmaceutical design. *Braz Arch Biol Technol*. 2007;50:63-76.
135. Suna X, Lia Y, Liua T, Lia Z, Zhanga X, Che X. Peptide-based imaging agents for cancer detection. *Adv. Drug Deliv. Rev.* 2017;110–111:38-51.
136. Wu X, Shaikh AB, Yu Y, et al. Potential diagnostic and therapeutic applications of oligonucleotide aptamers in breast cancer. *Int. J. Mol. Sci.* 2017;18(9):1851-1874.
137. Shi C, Zhu Y, Xie Z, et al. Visualizing human prostate cancer cells in mouse skeleton using bioconjugated near-infrared fluorescent quantum dots. *Urology*. 2009;74(2):446-451.
138. Barat B, Sirk SJ, McCabe KE, et al. Cys-diabody quantum dot conjugates (immunoQdots) for cancer marker detection. *Bioconjug. Chem.* 2009;20(8):1474-1481.

SUPPORTING INFORMATION

Additional supporting information may be found online in the Supporting Information section at the end of the article.

How to cite this article: Sengupta S, Asha Krishnan M, Chattopadhyay S, Chelvam V. Comparison of prostate-specific membrane antigen ligands in clinical translation research for diagnosis of prostate cancer. *Cancer Reports*. 2019;2:e1169. https://doi.org/10.1002/cnr2.1169